Received: 4 July 2023 | Revised: 17 November 2023 | Accepted: 11 December 2023

DOI: 10.1111/bph.16399

RESEARCH ARTICLE

ApTOLL: A new therapeutic aptamer for cytoprotection and (re)myelination after multiple sclerosis

Beatriz Fernández-Gómez[1,2,3] | Miguel A. Marchena[1,4,5] | David Piñeiro[2] | Paula Gómez-Martín[1] | Estefanía Sánchez[1] | Yolanda Laó[1] | Gloria Valencia[1] | Sonia Nocera[1] | Rocío Benítez-Fernández[1] | Ana M. Castaño-León[6] | Alfonso Lagares[6] | Macarena Hernández-Jiménez[2,7] | Fernando de Castro[1]

[1]Instituto Cajal—CSIC, Madrid, Spain

[2]AptaTargets SL, Madrid, Spain

[3]PhD Program in Neuroscience, Universidad Autónoma de Madrid—Cajal Institute, Madrid, Spain

[4]Facultad HM de Ciencias de la Salud de la Universidad Camilo José Cela

[5]Instituto de Investigación Sanitaria HM Hospitales

[6]Servicio de Neurocirugía, Hospital 12 de Octubre, Madrid, Spain

[7]Unidad de Investigación Neurovascular, Departamento de Farmacología y Toxicología, Facultad de Medicina, Universidad Complutense de Madrid, Madrid, Spain

Correspondence
Fernando de Castro, Instituto Cajal—CSIC, Avenida Doctor Arce 37, 28002 Madrid, Spain.
Email: fdecastro@cajal.csic.es

Present addresses
Sonia Nocera, University of California, San Francisco, California, USA; and Rocío Benítez-Fernández, Université de Fribourg, Fribourg, Switzerland.

Funding information
Programa de Doctorados Industriales, Comunidad de Madrid, Spain, Grant/Award Number: IND2018/BMD-9751; Ministerio de Ciencia e Innovación, Grant/Award Numbers: EIN2020-112366, PID2019-109858RB-I00, RD16/0015/0019, SAF2016-77575-R; Comunidad de Madrid; Ministerio de Ciencia

Abstract

Background and Purpose: ApTOLL is an aptamer selected to antagonize toll-like receptor 4 (TLR4), a relevant actor for innate immunity involved in inflammatory responses in multiple sclerosis (MS) and other diseases. The currently available therapeutic arsenal to treat MS is composed of immunomodulators but, to date, there are no (re)myelinating drugs available in clinics. In our present study, we studied the effect of ApTOLL on different animal models of MS.

Experimental Approach: The experimental autoimmune encephalomyelitis (EAE) model was used to evaluate the effect of ApTOLL on reducing the inflammatory component. A more direct effect on oligodendroglia was studied with the cuprizone model and purified primary cultures of murine and human oligodendrocyte precursor cells (OPCs) isolated through magnetic-activated cell sorting (MACS) from samples of brain cortex. Also, we tested these effects in an ex vivo model of organotypic cultures demyelinated with lysolecithin (LPC).

Key Results: ApTOLL treatment positively impacted the clinical symptomatology of mice in the EAE and cuprizone models, which was associated with better preservation plus restoration of myelin and oligodendrocytes in the demyelinated lesions of animals. Restoration was corroborated on purified cultures of rodent and human OPCs.

Conclusion and Implications: Our findings reveal a new therapeutic approach for the treatment of inflammatory and demyelinating diseases such as MS. The molecular nature of the aptamer exerts not only an anti-inflammatory effect but also neuroprotective and remyelinating effects. The excellent safety profile demonstrated by ApTOLL in animals and humans opens the door to future clinical trials in MS patients.

Abbreviations: CC, corpus callosum; CPZ, cuprizone; dpl, days post lesion; EAE, experimental autoimmune encephalomyelitis; haOPC, human adult oligodendrocyte precursor cell; LPC, lysolecithin; OPC, oligodendrocyte precursor cell; TLR4, toll-like receptor 4.

Macarena Hernández-Jiménez and Fernando de Castro contributed equally to this work.

Investigación e Innovación, Grant/Award Number: PID2022-143110OB-I00; Consejo Superior de Investigaciones Científicas, Grant/Award Number: 2019AEP033; AptaTargets SL, Grant/Award Number: ApTLR2019-PC-MS-001

KEYWORDS
aptamer, immunomodulation, myelin, neuroprotection, oligodendrocyte, OPC, TLR4

1 | INTRODUCTION

Multiple sclerosis (MS) is a primary demyelinating, chronic, neurodegenerative, inflammatory and autoimmune disease of the central nervous system (CNS). As in other primary demyelinating diseases, the main pathophysiological feature of MS is the loss of oligodendrocytes and myelin in the CNS, both in the white and grey matter (Trapp & Nave, 2008). This process is associated with the activation of macrophages and microglia, causing a background of inflammatory reactions (Baufeld et al., 2018). After damage, endogenous oligodendrocyte precursor cells (OPCs) spontaneously migrate to lesion sites, where they can differentiate into new myelin-forming mature oligodendrocytes (de Castro et al., 2013; Franklin & ffrench-Constant, 2017). The currently available treatments to manage MS are based on the use of immunosuppressive and immunomodulatory agents, although there is still no approved compound to successfully induce disease-reversing remyelination (Gudi et al., 2014; Kremer et al., 2015).

The family of **toll-like receptors** (TLRs) participates in innate immunity, modulating a wide variety of inflammatory responses. Specifically, **toll-like receptor 4** (TLR4) has been implicated in several pathologies with a significant inflammatory component, including MS (Bsibsi et al., 2002; Kerfoot et al., 2004; Zhang et al., 2019). TLR4 activation increases the expression and nuclear translocation of nuclear transcription factor kappa-B (NF-κB), leading to the release of proinflammatory cytokines such as **tumour necrosis factor-α** (TNF-α), **interleukin-1β** (IL-1β) or **interleukin-6** (IL-6), as well as chemokine and lymphocyte recruitment (Liu et al., 2017). In this regard, TLR4 inhibition is known to enhance the survival of oligodendrocytes and OPCs (Hayakawa et al., 2016; Taylor et al., 2010). Therefore, the possibility of downregulating immune responses with specific TLR4 antagonists, inhibiting specific intracellular proteins involved in these signalling pathways, has raised great interest. This is the case of ApTOLL (also called aptamer #4FT), an innovative antagonist selected against TLR4 with the potential to achieve an immunomodulatory and anti-inflammatory effect.

ApTOLL is a single-stranded DNA aptamer, selected using the systemic evolution of ligands by exponential enrichment (SELEX) technology. Aptamers offer several advantages over antibodies to make them ideal for future therapeutic applications, such as their high specificity and affinity and their ease to enter biological compartments given their small size and lack of immunogenicity, as well as their demonstrated safety in animals and humans (Zhou & Rossi, 2017). Based on its pharmacokinetic characteristics and its very low level of toxicity, ApTOLL has been positioned as a potential therapeutic option for the treatment of different diseases. In fact, ApTOLL has been successfully tested in preclinical models of ischaemic stroke and myocardial infarction, producing an excellent protective effect (Fernández et al., 2018; Paz-García et al., 2023; Ramirez-Carracedo et al., 2020). In clinical studies, ApTOLL has a very good safety profile in a completed first-in-human clinical trial in healthy subjects (Hernández-Jiménez et al., 2022) and has successfully completed a phase Ib/IIa trial (APRIL trial) to determine its safety and biological effects in acute ischaemic stroke patients (Hernández-Jiménez, Abad-Santos, Cotgreave, Gallego, Jilma, Flores, Jovin, Vivancos, Hernández-Pérez, et al., 2023; Hernández-Jiménez, Abad-Santos, Cotgreave, Gallego, Jilma, Flores, Jovin, Vivancos, Molina, et al., 2023).

In the present work, we demonstrate the beneficial effect of ApTOLL in the experimental autoimmune encephalomyelitis (EAE) and cuprizone (CPZ) models of MS. These in vivo results were completed with a detailed in vitro study of the effects of ApTOLL on primary cultures of OPCs, as well as the (de)myelination in organotypic cultures of cerebellar slices. Altogether, our present proof-of-concept study positions ApTOLL as a therapeutic agent to treat MS to obtain immunomodulatory, cytoprotective and neuroreparative effects.

What is already known

- ApTOLL offers protective effects and good safety profile in clinical trials in other diseases.

What does this study add

- ApTOLL decreased inflammation and promoted remyelination in different models of MS.

What is the clinical significance

- ApTOLL can act as a therapeutic agent to treat MS.

2 | METHODS

2.1 | Animals

Female and male C57/BL6 mice (7 weeks old) were purchased from Charles River Laboratories (Wilmington, MA, USA). Animals used in *in vivo* studies were transferred to the animal facility of the Instituto

Cajal—CSIC, where the mice were acclimatized for a week under the appropriate environmental conditions with ad libitum access to food and water prior to performing experimental procedures. Animals were randomly and blindly distributed into different groups designed to be of equal size and sufficient for comparison prior to treatment designation; however, in some cases, the groups were unequal due either to unexpected loss of mice or no illness in the EAE model. P7 Wistar rats from the animal facility of the Instituto Cajal—CSIC were used for primary cultures. All experimental procedures were performed in accordance with European Council Guidelines (63/2010/EU) and Spanish National and Regional Guidelines for Animal Experimentation and Use of Genetically Modified Organisms (RD 53/2013 and 178/2004, Ley 32/2007 and 9/2003, Decree 320/2010). The generation of different MS models was approved by the relevant institutional and regional ethics committees of CSIC (440/2016, Madrid, Spain). Animal studies are reported in compliance with the ARRIVE guidelines (Percie du Sert et al., 2020) and with the recommendations made by the *British Journal of Pharmacology* (Lilley et al., 2020).

2.2 | Induction of active EAE

EAE was induced in female mice (Melero-Jerez et al., 2021). Briefly, the mice were anaesthetized with 40 µl of an anaesthetic/analgesic solution containing **ketamine** (40 mg·ml^{-1}: Anesketin) and **xylazine** (2 mg·ml^{-1}: Rompun) injected intraperitoneally (i.p.). An emulsion of myelin oligodendrocyte glycoprotein (MOG_{35-55} peptide, 250 µg in a final volume of 200 µl: GenScript) and complete Freund's adjuvant containing inactivated *Mycobacterium tuberculosis* (4 mg: BD Biosciences) was introduced subcutaneously into animals' groin and armpits. Next, pertussis toxin (400 ng per mouse: Sigma-Aldrich) was administered intravenously (i.v.) through the tail vein on the day of immunization and 48 h later. The animals used as controls for the validation of the EAE model (the sham group) were immunized in the same way except for MOG_{35-55} peptide, which was replaced by sterile phosphate-buffered saline (PBS). The mice were weighed and evaluated double-blind on a daily basis until killed, scoring the animals as follows: 0, asymptomatic; 1, loss of muscle tone throughout the tail; 2, weakness or unilateral partial hind limb paralysis; 3, bilateral paralysis of the hind limbs; 4, tetraplegia; and 5, death. In all cases, mice were killed 10 days after the onset of symptoms.

2.2.1 | ApTOLL treatment

ApTOLL (0.45, 0.91, 1.82 or 3.6 mg·kg^{-1}, diluted in sterile PBS - 1 mM $MgCl_2$) or vehicle (PBS - 1mM $MgCl_2$) was administered i.v. to mice through a single injection at the onset of the symptoms (defined as a clinical score between 0.5 and 1.5) randomly. For the study of the therapeutic window, independent groups were established, and a single 0.91 mg·kg^{-1} dose was injected 24 h after the onset and at the peak of the symptoms. In all cases, the animals were evaluated for 10 days after onset.

2.3 | CPZ-induced model

Male, 8-week-old C57/BL6 mice were randomly separated into three groups: control-untreated, ApTOLL-treated, and vehicle-treated. While the control animals received a normal diet, the remainder of the mice were fed with chow containing CPZ (bis(cyclohexanone) oxaldihydrazone: Sigma-Aldrich) at 0.25% (w/w) ad libitum for 6 weeks, as previously described (Medina-Rodríguez et al., 2017). This copper chelator induces apoptosis in mature oligodendrocytes, which leads to robust demyelination, particularly in the corpus callosum (CC; Gudi et al., 2014). The body weight of each mouse was measured weekly, and ApTOLL or the vehicle alone was injected i.v. once weekly from the beginning of the experiments to the time of killing. To study CPZ-induced oligodendroglial proliferation, we add 5-ethynyl-2′-deoxyuridine (EdU; Invitrogen), a direct measure of de novo DNA synthesis, into the drinking water at 0.2 mg·ml^{-1} the week before killing. Finally, to assess remyelination, CPZ was removed from the diet at the end of the sixth week and animals were fed with normal chow for two more weeks (6 + 2 weeks). The treatment (vehicle or ApTOLL at 0.91 mg·kg^{-1}) was injected once a week after CPZ withdrawal, based on the fact that a single dose of ApTOLL has demonstrated strong effects in reducing inflammation for long times in experimental models of ischaemia (Fernández et al., 2018; Ramirez-Carracedo et al., 2020), as well as in the described weekly dependent pattern of inflammatory response and oligodendrocyte maturation and survival expression genes in the CPZ model after the sixth week (Gharagozloo et al., 2022; Zhang et al., 2022).

2.3.1 | Motor coordination test (rotarod)

At the end of the 6-week experimental period, animals were tested on a rotarod to evaluate their locomotor coordination. For training, mice were subjected to pre-test trials the day before, placing them on the rod at constant speed (30 r.p.m.). Each mouse performed the pre-test twice under the same conditions, and the latency to fall was measured. The distribution of the animals for the different experimental groups (ApTOLL/vehicle) was conducted in a double-blinded way. Animals for all groups were collected from the same boxes (same housing conditions) and the same provider, being animals from the same litter. With this approach, we avoided the undesirable variability among experiments as well as the possibility of including differences in animal skills.

2.4 | Tissue sampling

Animals were killed by i.p. administration of a lethal dose of **pentobarbital**, and perfused transcardially with 4% paraformaldehyde (PFA) in 0.1-M phosphate buffer (PB, pH 7.4). The brain and spinal cord were excised and post-fixed in 4% PFA for 4 h at room temperature (RT). The tissue was cryoprotected by immersion in an increasing sucrose gradient, and coronal cryostat sections (20 µm) were obtained using a CM1900 cryostat (Leica).

2.5 | Eriochrome cyanine (EC) staining

To analyse CNS demyelination, EC staining was performed as described previously (Medina-Rodríguez et al., 2017). In brief, the histological sections were dried for 2 h at RT and for 2 h at 37°C before being immersed in acetone for 5 min, dried and submerged in the EC solution (Sigma) for 30 min. To differentiate the samples, iron alum at 5% (w/v) was used for 5–10 min followed by a second differentiation step with borax-ferricyanide solution for 5 min at RT. For conservation, the sections were dehydrated in ethanol solutions of increasing concentration and mounted with a mounting medium (DPX, Sigma).

2.6 | Immunohistochemistry in CNS tissue

To detect antigens present in the spinal cord of EAE mice and the CC from CPZ-treated animals, sections were first pre-treated with 10% methanol in 0.1-M PB at RT for 15 min, and after several washes with 0.1-M PB and PB saline (PBS), they were incubated for 1 h at RT with blocking solution to avoid non-specific binding: 5% of normal donkey serum (NDS) and 0.02% of Triton X-100 (Sigma-Aldrich) in PBS. The sections were then incubated overnight at 4°C with the primary antibodies (1:1000 rabbit polyclonal anti-NFH [Abcam, Cat# ab8135, RRID:AB_306298]; 1:500 guinea pig monoclonal anti-Iba1 [Synaptic Systems, Cat# 234308, RRID:AB_2924932]; 1:200 mouse monoclonal anti-CC1 [Millipore, Cat# OP80, RRID:AB_2057371]; 1:200 goat polyclonal anti-**PDGFRα** [R&D Systems, Cat# AF1062, RRID:AB_2236897]; 1:900 rabbit polyclonal anti-Caspr [Abcam, Cat# ab34151, RRID:AB_869934]; 1:500 mouse monoclonal anti-GFAP [Millipore, Cat# MAB3402, RRID:AB_94844]; 1:250 mouse monoclonal anti-CD68 [Thermo Fisher, Cat# 14-0688-82, RRID:AB_11151139]; 1:200 goat polyclonal anti-CD206 [Thermo Fisher, Cat# PA5-46994, RRID:AB_2607366]; 1:500 rat monoclonal anti-MBP [Bio-Rad, Cat# MCA409S, RRID:AB_325004]; and 1:200 rabbit polyclonal anti-Olig2 [Millipore, Cat# AB9610, RRID:AB_570666]) (Table 1); after washing, they were probed for 1 h at RT with fluorescent secondary antibodies. The secondary antibodies used were as follows: 1:1000 Alexa Fluor 488 donkey anti-rat IgG (A-21208, Thermo Fisher); 1:1000 Alexa Fluor 488 donkey anti-goat IgG (A-11055, Thermo Fisher); 1:1000 Alexa Fluor 488 goat anti-guinea pig IgG (A-11073, Thermo Fisher); 1:1000 Alexa Fluor 594 donkey anti-rat IgG (A-21209, Thermo Fisher); 1:1000 Alexa Fluor 568 donkey anti-rabbit IgG (A10042, Thermo Fisher); 1:1000 Alexa Fluor 647 donkey anti-rabbit IgG (A-31573, Thermo Fisher); and 1:1000 Alexa Fluor 647 donkey anti-mouse IgG (A-31571, Thermo Fisher). Cell nuclei were stained with Hoechst 33342 (10 $\mu g \cdot ml^{-1}$: Sigma-Aldrich) and, finally, the tissue was washed and mounted with Fluoromount® mounting medium (SouthernBiotech). We also used FluoroMyelin Green fluorescent myelin stain (Invitrogen) for quick and selective labelling of myelin in brain cryosections. As such, the samples were rehydrated with PBS and incubated with the staining solution for 20 min at RT. Subsequently, the sections were rinsed in PBS three times and mounted with Fluoromount®. To visualize cell proliferation, an EdU detection cocktail (Click-iT EdU Alexa Fluor 488 HCS assay, Invitrogen) was used according to the manufacturer's instructions. The Immuno-related procedures used comply with the recommendations made by the *British Journal of Pharmacology* (Alexander et al., 2018).

2.7 | Primary OPC cultures

OPCs from the cerebral cortex of P7 Wistar rats and P7 mice (C57/BL6) were isolated using magnetic-activated cell sorting (MACS) (Miltenyi; Dincman et al., 2012; Melero-Jerez et al., 2021). First, the animal's brain was extracted, and then the meninges were removed in a Petri dish containing cooled Hank's balanced salt solution with Ca^{2+} and Mg^{2+} ($HBSS^{+/+}$: Gibco) to maintain OPC metabolism. According to the manufacturer's instructions, the brain cortices were then mechanically triturated in $HBSS^{-/-}$ and enzymatically digested for 25 min at 37°C with enzymes provided in the Neural Tissue Dissociation Kit (P) (Miltenyi) under mild and continuous agitation. After adding the second mix, the tissue was dissociated using a 5-ml pipette. The suspension was passed through a 70-μm nylon cell strainer (BD Falcon), centrifuged at 300 *g* for 10 min and incubated for 25 min at 4°C with the primary antibody for A2B5 (Millipore) and/or O4 hybridoma cells (Developmental Studies Hybridoma Bank [DSHB], Iowa) diluted 1:1 in Miltenyi wash buffer (MWB—2-mM sodium pyruvate, 0.5% bovine serum albumin [BSA] and 2-mM ethylenediaminetetraacetic acid [EDTA] adjusted to pH 7.3). Thereafter, cells were washed with MWB and exposed to the secondary rat anti-mouse IgM antibody (anti-mouse IgM microbeads: Miltenyi) for 15 min at 20 $\mu l/10^7$ cells. Next, the cell suspensions were washed and passed through an MWB-coated medium-size column (MS, Miltenyi) coupled to a magnet and eluted with Neuro Medium (Miltenyi) supplemented with 2% MACS® NeuroBrew-21 w/o vitamin A (Miltenyi), 0.6% penicillin/streptomycin (10,000-U·ml^{-1} penicillin and 10-mg·ml^{-1} streptomycin: Sigma), glutamine (200 mM, Gibco), D-glucose (25 mM, Normapur) and 10 ng·ml^{-1} of **platelet-derived growth factor-AA** (PDGF-AA: Merck) and **fibroblast growth factor-2** (FGF-2: PeproTech). Finally, the cells were counted and seeded on coverslips coated with poly-L-lysine (0.1 mg·ml^{-1} in borate buffer, pH 8.5: Sigma) and laminin (10 μg·ml^{-1} in PBS: Sigma). A purity of ~90% was obtained.

Human adult OPCs (haOPCs) were isolated from biopsies of the adult cerebral cortex following surgery in traumatic brain injury patients, obtained from the Neurosurgery Service of the Hospital 12 de Octubre (Madrid) and conserved immediately in Hibernate-A (Gibco) at 4°C up to the isolation process. The study was conducted according to the guidelines and the Research Ethics Committee-approved protocol of the Instituto Cajal—CSIC (440/2016 and 2016/049/CEI3/20160411) and CSIC (073/2021). To obtain OPC cells, the same procedure as above was applied with some modifications. After filtration, the pellet was passed through a 20% Percoll (GE HealthCare) gradient and centrifuged at 800 *g* for 20 min. The cells were then exposed to a Red Blood Cell Removal Solution (Miltenyi) diluted in ddH_2O for 10 min at 4°C. An anti-O4 MicroBead

TABLE 1 List of primary antibodies used.

Use	Antibody	Target	Dilution	Species	Supplier
IHC	NFH	Neurofilaments	1:1000	Rabbit (polyclonal IgG)	Abcam (Cat# ab8135, RRID:AB_306298)
IHC	Iba1	Microglia	1:500	Guinea pig (monoclonal IgG)	Synaptic Systems (Cat# 234308, RRID:AB_2924932)
IHC	CC1	Mature oligodendrocytes	1:200	Mouse (monoclonal IgG)	Millipore (Cat# OP80, RRID:AB_2057371)
IHC	PDGFRα	OPCs	1:200	Goat (polyclonal IgG)	R&D Systems (Cat# AF1062, RRID:AB_2236897)
IHC	Caspr	Paranodes	1:900	Rabbit (polyclonal IgG)	Abcam (Cat# ab34151, RRID:AB_869934)
IHC	GFAP	Astrocytes	1:500	Mouse (monoclonal IgG)	Millipore (Cat# MAB3402, RRID:AB_94844)
IHC	CD68	Macrophages and microglia with phagocytic activity	1:250	Mouse (monoclonal IgG)	Thermo Fisher (Cat# 14-0688-82, RRID:AB_11151139)
IHC	CD206	Anti-inflammatory microglia	1:200	Goat (polyclonal IgG)	Thermo Fisher (Cat# PA5-46994, RRID:AB_2607366)
IHC/ ICC	MBP	Myelin	1:500	Rat (monoclonal IgG)	Bio-Rad (Cat# MCA409S, RRID:AB_325004)
IHC/ ICC	Olig2	Oligodendroglial lineage	1:200	Rabbit (polyclonal IgG)	Millipore (Cat# AB9610, RRID:AB_570666)
ICC	BrdU	Proliferating cells	1:1000	Rat (monoclonal IgG)	Abcam (Cat# ab6326, RRID:AB_305426)

Abbreviations: ICC, immunocytochemistry; IHC, immunohistochemistry; OPCs, oligodendrocyte precursor cells.

antibody (2.5 µl: Miltenyi) was resuspended in 97.5 µl of MWB and used to label up to 10^7 total cells by incubating for 15 min at 4°C in the dark with mild agitation. Culture purity was at least 85%. Due to the intrinsic difficulties of obtaining neurosurgical samples from adult human tissue, as well as isolating viable haOPCs from these usually small biopsies and the lower survival rate of haOPCs compared to those isolated from rodents, the number of valid independent experiments in the present work was less than 5. Therefore, although exploratory, we consider the inclusion of these results interesting because of their potential relevance for future clinical translation.

2.7.1 | Viability/survival assay

The viability of the OPCs after the different treatments was tested with a thiazolyl blue tetrazolium bromide (MTT) assay that measured the mitochondrial activity of the cells by quantifying the conversion of the tetrazolium salt to its formazan product. Cells were seeded in 96-well plates at a density of 15,000 cells per well in a final volume of 200 µl and treated the day after the culture with ApTOLL (20 and 200 nM), the vehicle alone or 5% H_2O_2 as a cell death control. After 24 h, MTT (5 mg·ml^{-1}: Sigma) was added to the plates, and the cells were left in the incubator for 4 h, after which the medium was removed, dimethyl sulfoxide (DMSO; Invitrogen) was added to dissolve the formazan formed, and the absorbance of this solution was measured. Likewise, the survival of OPCs was determined by terminal deoxynucleotidyl transferase dUTP nick-end labelling (TUNEL) staining (see Melero-Jerez et al., 2021). To this end, the cells were seeded in 24-well plates at 30,000 cells per coverslip in a final volume of 500 µl, treated with ApTOLL or its vehicle alone on the following day and then fixed in 4% PFA after 48 h.

2.7.2 | Proliferation assay

To analyse OPC proliferation, the cells were seeded, as previously described, at a density of 30,000 cells per coverslip (Melero-Jerez et al., 2021) and, after 24 h, the medium was replaced with medium containing the corresponding treatments. A pulse of 5-bromo-2-deoxyuridine (BrdU, 50 µM; Sigma-Aldrich) was given to the neonatal cells for 6 h (from 24 to 30 h in vitro). At the end of this time, the medium was refreshed and the cells were fixed in 4% PFA on the following day.

2.7.3 | Differentiation assay

Cells were seeded at 30,000 cells per coverslip, and 24 h later, the medium was replaced with a new medium without growth factors (PDGF-AA and FGF-2). The following day, the treatments were added, and the cells were fixed and immunolabelled at the end of the fifth day in vitro.

2.8 | Immunocytochemistry of in vitro cultures

After fixing the cells with 4% PFA, they were washed with PBS and maintained for 1 h under shaking in the blocking solution (5% NDS and 0.02% Triton X-100). The cells were then incubated overnight with the corresponding primary antibodies (anti-MBP, anti-Olig2, anti-CC1 and 1:1000 rat monoclonal anti-BrdU [Abcam, Cat# ab6326, RRID:AB_305426]) in a humid chamber at 4°C and, after washing, exposed to secondary antibodies for 1 h at RT in the dark. The nuclei were stained with Hoechst (1:20) for 10 min in the dark, and the coverslips were mounted in Immu-Mount (Thermo Fisher).

To study proliferation, BrdU labelling was performed after Olig2 staining. After washing the cells, they were denatured with HCl 2 N for 45 min at RT, washed with borate buffer and blocked for 3 h at RT with PBS containing 5% fetal bovine serum (FBS), 0.03% Triton X-100, 0.2% gelatine and 0.2-M glycine. They were then incubated overnight at 4°C with an anti-BrdU rat antibody (Abcam) diluted in blocking solution, and after several washes, they were exposed to the secondary antibody for 4 h before Hoechst staining. TUNEL staining was performed with the ApopTag Plus Fluorescein In Situ Apoptosis Kit (Merck Millipore, Sigma-Aldrich) following the manufacturer's instructions. Briefly, cells were equilibrated with the corresponding buffer and incubated for 1 h at 37°C in 50% terminal deoxynucleotidyl transferase (Tdt) in reaction buffer. The reaction was stopped, and after washing, the coverslips were exposed for 30 min to 47% anti-digoxigenin diluted in the blocking buffer. Finally, the standard protocol was applied to label additional markers.

2.9 | Organotypic cultures of cerebellar slices

Cerebellar slices from neonatal wild-type (WT) mice were cultured following standard protocols (Birgbauer et al., 2004; Medina-Rodríguez et al., 2017; Melero-Jerez et al., 2021). In brief, mice were decapitated and their brain and cerebellum were deposited in a Petri dish filled with $HBSS^{+/+}$ and on ice. The cerebellum was separated, immediately placed on a Teflon base and cut automatically into 350-µm slices on a McIlwain Tissue Chopper (Mickle Laboratory Engineering Co. Ltd). Cerebellar parasagittal slices were transferred under sterile conditions to 30-mm-diameter Millicell inserts with a pore size of 0.4 µm (Millipore), placed in a six-well plate with 1 ml of culture medium consisting of 25% $HBSS^{+/+}$, 50% Basal Medium Eagle (BME: Gibco), 25% inactivated horse serum (Gibco), 28-mM D-glucose, 1% penicillin/streptomycin solution and 0.25-mM GlutaMAX (Gibco). The medium was refreshed every other day, and a demyelinating toxin, **lysolecithin** (LPC, 0.5 $mg \cdot ml^{-1}$: Sigma), was added after 7 days in vitro (DIV) for 15 h. Subsequently, the medium was removed, and the slices were treated with ApTOLL (20 nM) or the vehicle alone in fresh culture medium. The cultures were maintained until 6 days post-lesion (dpl), refreshing the medium and treatment every other day, fixing samples with 4% PFA for 15 min at both 0 dpl as an internal control for the effectiveness of LPC and 6 dpl. Finally, cultures were stained for myelin basic protein (MBP), neurofilament heavy chain (NFH) and Iba1 as described above.

2.10 | Image and data analysis

Optical images of EC staining were acquired, and mosaics were built using the bright-field camera of a THUNDER microscope (Leica) at 20× and 40× magnification. Fluorescence images of tissue samples were taken on an inverted Leica SP-5 confocal microscope at the Microscopy and Image Analysis Unit of the Instituto Cajal—CSIC. In the EAE model, mosaics of three spinal cord samples were obtained per animal at 40× magnification and at a resolution of 512 × 512 pixels, with a separation between *z* planes of 3 µm. Demyelinated areas and MBP/NFH staining were assessed using the ImageJ application, and the cell counts were analysed with the microscopy software for 3D and 4D Imaging (IMARIS). The results of the analysis of these markers are shown in the graphs with respect to the mean value of the vehicle. Similarly, the central zone of the CC was evaluated in the CPZ model. Images were acquired with the same confocal microscope at a 40× magnification (for Caspr labelling a 63× objective was used), at a resolution of 1024 × 1024 pixels and with a separation of 0.5 µm between the *z* planes. The same parameters were applied for microphotographs of cerebellar slices, including a digital zoom of 1.7. The quantification of the different markers was performed using ImageJ software. Images of primary cultures were obtained using a Leica AF 6500-7000 microscope (five random photos per coverslip at 20× magnification), and cells were counted manually with the LAS X Life Science software. The absorbance for the viability assay was measured with a fluorometer FLUOstar OPTIMA (BMG Labtech) at 595 nm.

2.10.1 | Morphometric analysis of microglia

We studied the morphological complexity of microglia, to determine their functionality in organotypic slices under inflammatory conditions (when exposed to LPC). A minimum of 10 cells per condition were randomly analysed and processed with ImageJ software, following the previously published protocol (Young & Morrison, 2018). In summary, for the skeleton analysis, the image was first adjusted for brightness/contrast if necessary and processed to remove background noise. It was then converted to a binary image, and the AnalyzeSkeleton (2D/3D) plugin was run.

2.11 | Materials

Details of materials and suppliers are provided in specific subsections in Methods.

2.12 | Statistical analysis

The data and statistical analysis comply with the recommendations of the *British Journal of Pharmacology* on experimental design and analysis in pharmacology (Curtis et al., 2022). The data are expressed as the means ± SEM throughout, and they were analysed with GraphPad (GraphPad Software, La Jolla, CA, USA). In the text, (*n*) represents biological replicates; each *n*-value denotes individual mice or independent experiments. Statistics were undertaken for studies where each group size was at least n = 5. First, a D'Agostino and Pearson normality test was used to check if the values followed a Gaussian distribution. To compare pairs of independent groups, the Student's *t*-test was used or the Mann–Whitney *U*-test used for non-parametric data. The comparison of the clinical score between two treated groups (EAE-Veh and EAE-ApTOLL) was performed on each day from onset to the time of animal killing (10 days after onset) using Student's *t*-test. For multiple comparisons, a one-way analysis of variance (ANOVA) test was carried out in conjunction with the corresponding post hoc tests (if the ANOVA was significant): Tukey's test for parametric samples and Dunn's test for non-parametric samples. The threshold for statistical significance is set at $P < 0.05$.

2.13 | Nomenclature of targets and ligands

Key protein targets and ligands in this article are hyperlinked to corresponding entries in https://www.guidetopharmacology.org and are permanently archived in the Concise Guide to PHARMACOLOGY 2021/22 (Alexander et al., 2021).

3 | RESULTS

3.1 | ApTOLL treatment reduces EAE severity and demyelination in the spinal cord

For EAE, a T cell-driven inflammation and demyelination model of the highly inflammatory early phase of MS (Lassmann & Bradl, 2017), we determined the optimal dose of ApTOLL for reducing the clinical score by assessing four different concentrations (0.45, 0.91, 1.82 and 3.6 $mg{\cdot}kg^{-1}$; Fernández et al., 2018), administered through a single i.v. injection at the onset of EAE symptoms. The recovery of the clinical scores reached was significantly lower when the two intermediate doses were used. Differences between the EAE-Veh and EAE-ApTOLL-treated groups were observed from the beginning of the treatment, because there was a clear reduction in the slope of the curve and the disease scores obtained for the latter were significantly lower from Day 4 onwards (Figure 1a). The EAE-ApTOLL-treated mice showed a high recovery rate at the endpoint compared with the vehicle mice (dose 0.91 $mg{\cdot}kg^{-1}$: 67.2 ± 2.4%; dose 1.82 $mg{\cdot}kg^{-1}$: 66.7 ± 7.9%) or with their own clinical scores at the peak of the disease (ApTOLL recovery at the endpoint vs. peak: 61.8 ± 4.9% for the dose 0.91 $mg{\cdot}kg^{-1}$ and 60.6 ± 5.8% for the dose 1.82 $mg{\cdot}kg^{-1}$). Importantly, the sham group did not present any pathological manifestations in these studies.

The histological study showed significantly less demyelination after administration of the 0.91 and 1.82 $mg{\cdot}kg^{-1}$ doses. In accordance with these results, EAE-ApTOLL-treated animals had fewer and relatively smaller demyelinated lesions (mainly ventrolateral) in the white matter than in EAE-Veh mice (Figure 1b). Indeed, the total demyelination diminished significantly (by at least 75%) in the animals that received ApTOLL (Figure 1c). These results were in line with data obtained from the areas of well-preserved myelin and neurofilaments (expressing MBP and NFH, respectively) that were larger in EAE-ApTOLL-treated animals than in EAE-Veh animals (data normalized with respect to the EAE-Veh group; Figure 1d,e). In addition, an increase in the number of cells of oligodendroglial lineage ($Olig2^+$ cells) was observed following ApTOLL treatment (Figure 1f,g), although the effects were particularly noticeable for OPCs ($PDGFR\alpha^+/Olig2^+$ cells) and mature oligodendrocytes ($CC1^+/Olig2^+$ cells: Figure 1g). The comparison between these two doses for all these markers led us to choose the dose of 0.91-$mg{\cdot}kg^{-1}$ ApTOLL as optimal for our purposes (and used in the rest of our study).

Similarly, we determined the therapeutic window for the single dose of ApTOLL. Although there was a reduction in clinical severity in each of these three treatment groups, the effects of ApTOLL were strongest when it was administered at the onset of the EAE symptoms and 24 h after onset, but not at the peak reached by the clinical score (Figure 2a). Demyelination was significantly lower in the three groups treated with ApTOLL when compared with EAE-Veh animals, although this effect was particularly stronger when this agent was administered at the onset of EAE symptoms (Figure 2b,c), as it was in general for the rest of the histological parameters studied (Figure 2d–g). Altogether, we decided to choose the onset as the moment to treat the animals for the rest of our study.

3.2 | Treatment with ApTOLL decreases inflammation in the murine EAE model

Because inflammation is one of the main characteristics of MS, and due to the central role of TLR4 in the activation of microglia, we determined the presence of $Iba1^+$ cells in the spinal cord of EAE mice that had been injected with ApTOLL at the onset of symptoms. A significant decrease was detected for $Iba1^+$ cells, to approximately half the number of these inflammatory cells, especially in the lesion areas (Figure 3a,b). To identify different microglial/macrophage states within demyelinating lesions of EAE mice, we used CD68 to recognize microglia/macrophages reactive to damage and CD206 to identify a maintenance/repair phenotype (Paolicelli et al., 2022). We observed

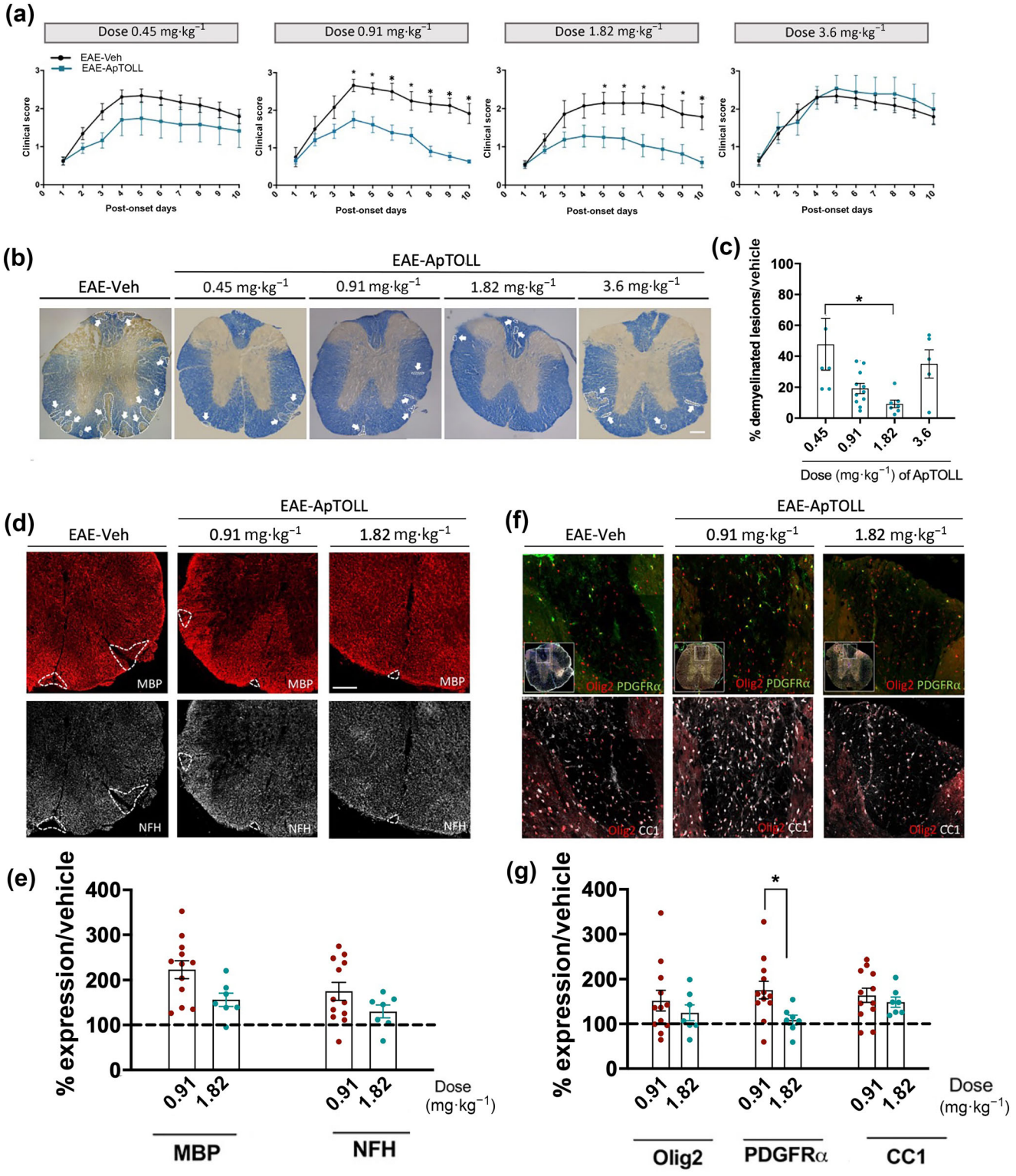

FIGURE 1 Legend on next page.

that ApTOLL-treated animals expressed significantly less microglia/macrophages in a reactive state but more in a reparative state (Figure 3c–e). Moreover, this process that seemed to be favoured by the shift of these cells towards repair phenotypes was noticed through their morphology (larger number and longer length of branches) (Orihuela et al., 2016), after exposure to a demyelinating insult and subsequent treatment with ApTOLL (Figure S1).

3.3 | ApTOLL also promotes myelin preservation and remyelination in the murine CPZ model of MS

To better evaluate the effects of ApTOLL on oligodendroglial biology, we took advantage of the CPZ in vivo model, because this copper chelator induces reversible demyelination in the CNS, particularly in the CC (Kipp et al., 2009). Mice were maintained on a CPZ diet for 6 weeks with a weekly dose of ApTOLL throughout (Figure 4a). Because myelin destabilization and loss in the CC begin to be evidenced 2–3 weeks after CPZ administration, accompanied by robust astrogliosis and microgliosis in this model, we therefore aimed to study the effect of ApTOLL on these last two processes in an acute phase. While inflammation (Figure S2A,B) and astrogliosis (Figure S2C,D) decreased in the ApTOLL-treated animals, OPC proliferation at the end of Week 3 (by quantifying the co-immunolabelling of Olig2 -oligodendroglial lineage- and EdU incorporation-proliferating cells; Gudi et al., 2014) was promoted (Figure S2E,F). After 6 weeks on the CPZ diet, when the peak of demyelination occurs (Hibbits et al., 2009), animals were tested using a rotarod. The motor coordination, as well as the latency to fall, were severely affected in the CPZ-Veh mice when compared with control mice, but the administration of ApTOLL improved their motor function, closely resembling the control animals (Figure 4b). In agreement with previous reports (Gudi et al., 2009; Skripuletz et al., 2008), a 6-week diet with CPZ induced almost complete loss of myelin in the CC in the CPZ-Veh group, while weekly ApTOLL injections partially protected this tissue against demyelination (Figure 4c,d). ApTOLL treatment also reflected a decrease in the density of both microglia/macrophages and GFAP-expressing astrocytes (Figure S2G–I). A role for this compound in the preservation of mature myelinated axons also was suggested by the number of nodes of Ranvier. While this number was markedly reduced in CPZ-Veh demyelinated animals, ApTOLL treatment doubled their number, although remaining significantly below the control group (Figure 4c,e). In addition, the number of OPCs was recovered after ApTOLL administration, and although the number of mature oligodendrocytes doubled with the treatment, they remained lower (just about one fourth) than in the control mice (Figure 4c,f,g). Finally, we studied the effect of ApTOLL on remyelination 2 weeks after the removal of CPZ from the diet (6 + 2 weeks; Figure 4h). These groups received treatment once a week after CPZ withdrawal and were fed with normal chow. Results showed an increase in both myelin area and the number of $CC1^+/Olig2^+$ cells in the CPZ-ApTOLL group (Figure 4i–k), suggesting a promotion of the remyelination process.

3.4 | ApTOLL treatment enhances OPC proliferation and differentiation in vitro without affecting their survival

The in vivo data obtained previously in these animal models of MS suggest that ApTOLL affects different pathogenic aspects, possibly including the promotion of spontaneous remyelination. To further elucidate whether ApTOLL would exert a direct effect on OPCs, we tested the effects of the aptamer at two different concentrations (20 and 200 nM, as tested previously by Fernández et al., 2018) on the survival, proliferation and differentiation of OPCs in purified primary cultures. Neither OPC viability in MTT assays (Figure S3A) nor their survival in TUNEL assays (Figure 5a,b) was affected by ApTOLL; however, exposure to this aptamer did significantly induce OPC proliferation (Figure 5c,d). Regarding the maturation of OPCs towards myelinating phenotypes and their myelin production, we maintained cells in culture for 5 days under different experimental conditions. Exposure to ApTOLL produced a significant increase not only in the number of mature oligodendrocytes expressing the MBP marker (Figure 5e,f) but also in the area occupied by this antibody relative to

FIGURE 1 ApTOLL dose–response study in EAE. (a) Clinical course of the animals treated with each dose of ApTOLL compared to vehicle groups. There is a significant reduction in the clinical score of EAE after the injection of ApTOLL at the time of the onset of symptoms, both at a dose of 0.91 and 1.82 $mg{\cdot}kg^{-1}$. Demyelinated areas are indicated with white arrows (b) and quantified with respect to the white matter area in each experimental group (c). The optimal doses for ApTOLL treatment in the murine EAE model of MS are the intermediate ones. (d, e) Images of the different markers in the lesions (dashed white lines): MBP (red) and NFH (grey) (d). Graphs representing the recovery rate of ApTOLL-treated mice relative to the vehicle group (MBP: dose 0.91 $mg{\cdot}kg^{-1}$ of EAE-Veh vs. EAE-ApTOLL, $P < 0.05$; dose 1.82 $mg{\cdot}kg^{-1}$ of EAE-Veh vs. EAE-ApTOLL, $P < 0.05$; NFH: dose 0.91 $mg{\cdot}kg^{-1}$ of EAE-Veh vs. EAE-ApTOLL, n.s.; dose 1.82 $mg{\cdot}kg^{-1}$ of EAE-Veh vs. EAE-ApTOLL, n.s.) (e). Magnified images (f) and histograms (g) of the oligodendrocyte studies at different stages of maturation (Olig2: dose 0.91 $mg{\cdot}kg^{-1}$ of EAE-Veh vs. EAE-ApTOLL, n.s.; dose 1.82 $mg{\cdot}kg^{-1}$ of EAE-Veh vs. EAE-ApTOLL, n.s.; PDGFRα: dose 0.91 $mg{\cdot}kg^{-1}$ of EAE-Veh vs. EAE-ApTOLL, $P < 0.05$; dose 1.82 $mg{\cdot}kg^{-1}$ of EAE-Veh vs. EAE-ApTOLL, n.s.; CC1: dose 0.91 $mg{\cdot}kg^{-1}$ of EAE-Veh vs. EAE-ApTOLL, $P < 0.05$; dose 1.82 $mg{\cdot}kg^{-1}$ of EAE-Veh vs. EAE-ApTOLL, n.s.). The 0.91 $mg{\cdot}kg^{-1}$ dose is optimal for ApTOLL treatment in EAE. Scale bar: 200 μm in (b), (d) and (f). EAE-ApTOLL n = 6, EAE-Veh n = 5 and control n = 5 for a dose of 0.45 $mg{\cdot}kg^{-1}$; EAE-ApTOLL n = 13, EAE-Veh n = 6 and control n = 10 for a dose of 0.91 $mg{\cdot}kg^{-1}$; EAE-ApTOLL n = 8, EAE-Veh n = 7 and control n = 8 for a dose of 1.82 $mg{\cdot}kg^{-1}$; and EAE-ApTOLL n = 5, EAE-Veh n = 5 and control n = 5 for a dose of 3.6 $mg{\cdot}kg^{-1}$. The clinical score data of the EAE-Veh and EAE-ApTOLL groups were compared by an unpaired Student's *t*-test on each day (from onset to time of sacrifice). Results of the one-way ANOVA with a Tukey's post hoc test and of the unpaired Student's *t*-test for two independent groups are represented by $^*P < 0.05$.

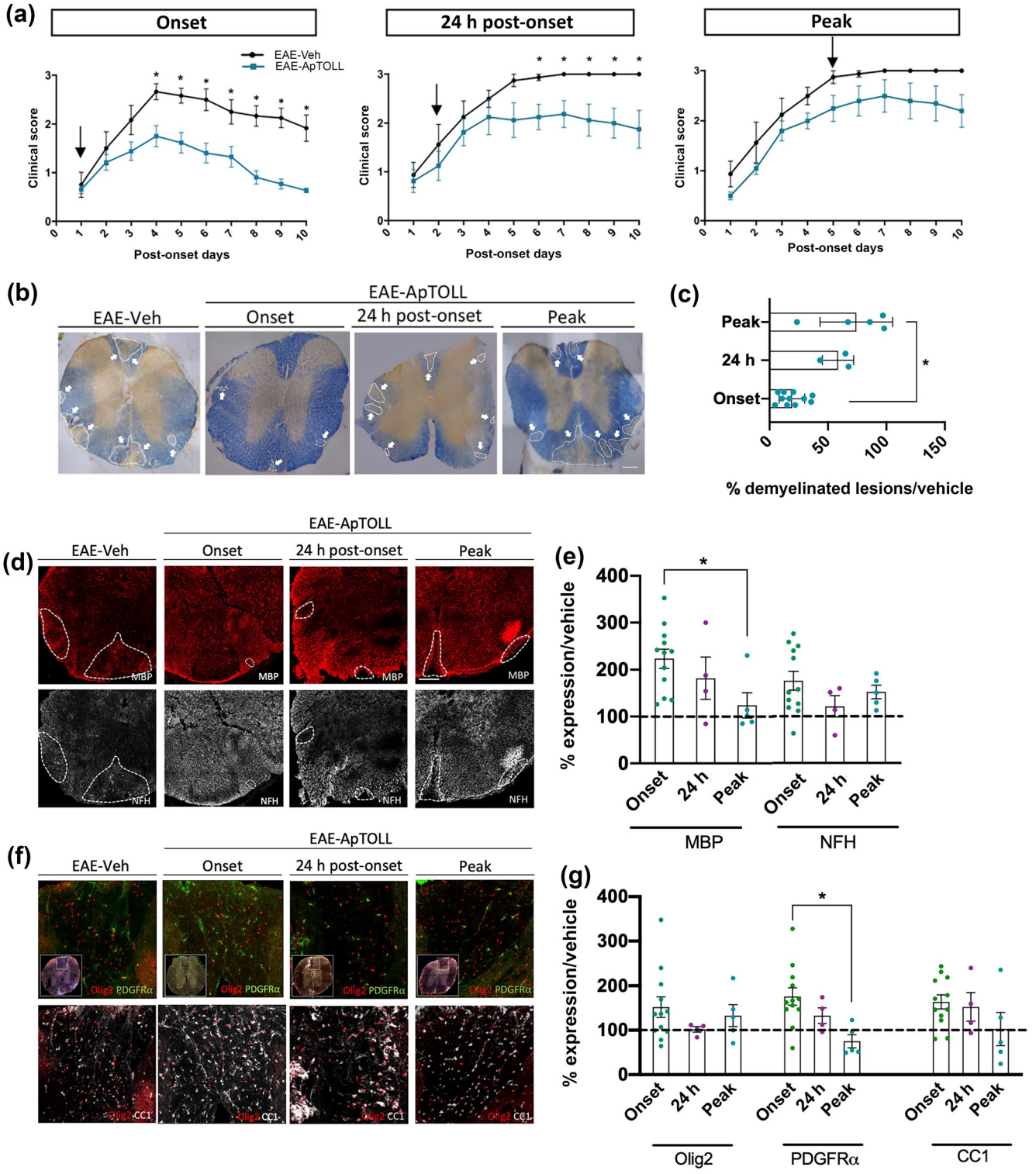

FIGURE 2 Determination of the therapeutic window with the optimal dose of ApTOLL. (a) Clinical course of the animals treated with ApTOLL at different time points of the disease relative to their respective vehicle group: onset (EAE-Veh n = 6; EAE-ApTOLL n = 13), 24 h after onset (EAE-Veh n = 4; EAE-ApTOLL n = 4) and peak (EAE-Veh n = 4; EAE-ApTOLL n = 5). Representative images of EC staining (b) and the quantification of demyelination relative to their respective vehicle group (c). White arrows indicate lesions. The treatment is more effective when injected at the onset of symptoms. Representative images (d) and a graphical representation of the recovery rate of MBP, NFH and Iba1 relative to the vehicle group (e). Representative magnification of the oligodendrocyte labelling at different stages of maturation (f) and a graph of the oligodendrocyte ratio at different times of injection (g). Scale bar: 200 μm in (b), (d) and (f). The clinical score data of the EAE-Veh and EAE-ApTOLL groups were compared by an unpaired Student's *t*-test on each day (from onset to time of sacrifice). The results of the one-way ANOVA with a Dunn's post hoc test are represented by $^*P < 0.05$.

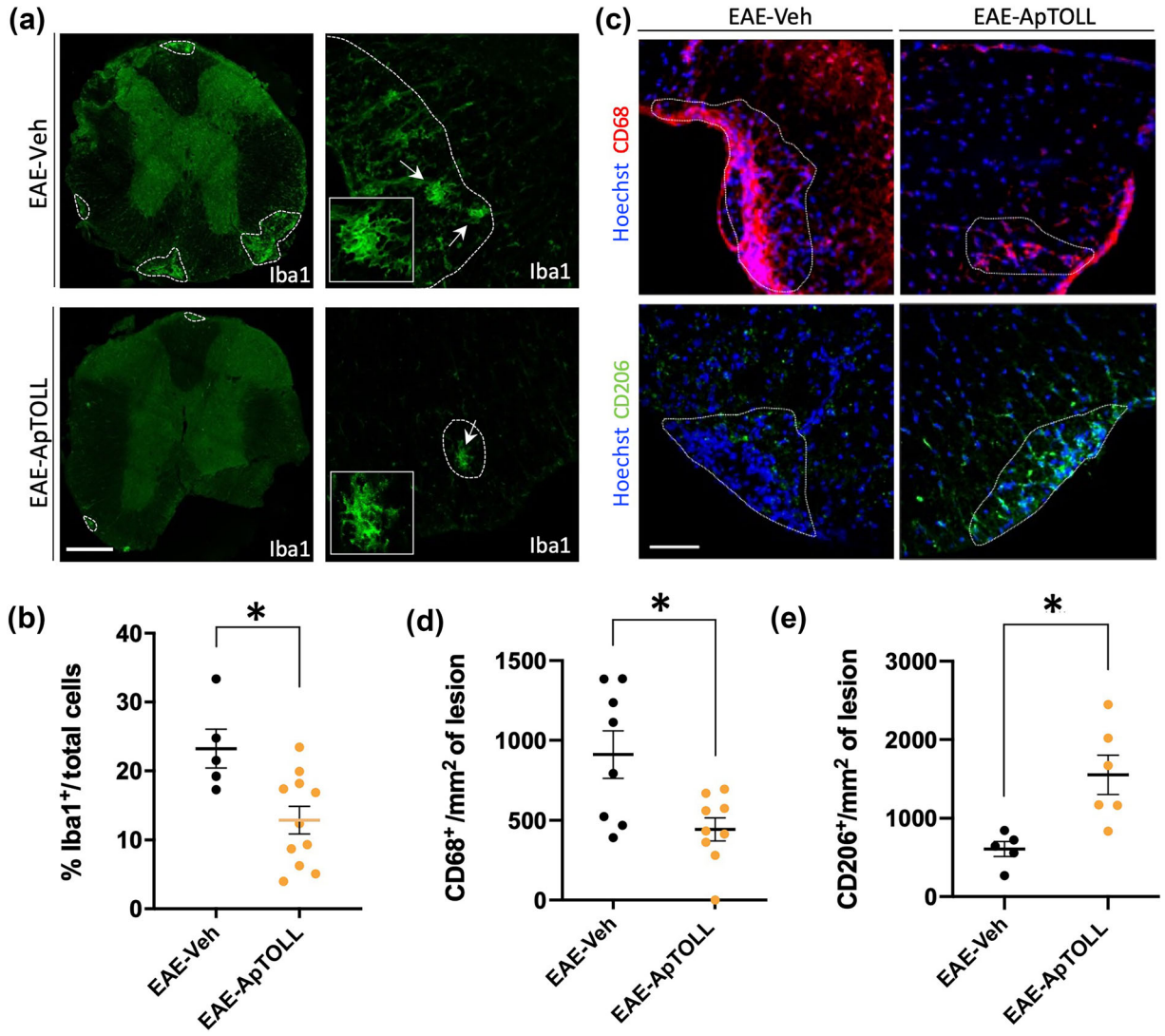

FIGURE 3 ApTOLL treatment reduces Iba1$^+$ cells in EAE mice lesions and induces an anti-inflammatory transformation of microglia/macrophages. (a) Representative images and magnifications of the lesions showing Iba1$^+$ labelling. (b) Quantification of the microglial/macrophage cells in the spinal cord. A significant reduction was observed following the ApTOLL treatment. (c) Representative images of the main microglia markers: CD68 to recognize activated microglia in red fluorescence and CD206 commonly used to identify anti-inflammatory phenotypes in green fluorescence. Histograms showing a significant decrease in CD68 expression (d) and an increase in CD206 (e). Scale bar: 60 µm in (a) and (c) and 20 µm in magnifications. An unpaired Student's *t*-test was used to compare the groups: $^*P < 0.05$.

the control OPCs (MBP$^+$ area in Veh 4711 ± 1402 µm^2, in ApTOLL [20 nM] 8082 ± 757 µm^2 and in ApTOLL [200 nM] 9871 ± 1415 µm^2: one-way ANOVA Dunn's post hoc test Veh vs. ApTOLL [20 and 200 nM] $P < 0.05$). Similar results were obtained in murine OPCs (Figure S3B–H). Accordingly, we concluded that ApTOLL exerts a direct pro-myelinating role in vitro.

3.5 | ApTOLL promotes remyelination ex vivo

To study the impact of ApTOLL on myelin regeneration after a demyelinating insult, ex vivo organotypic cerebellar slice cultures were prepared from neonatal mice and tissue damage was evoked with LPC, a membrane-disrupting chemical that provokes rapid loss of myelin and oligodendrocytes (Figure 6a; Birgbauer et al., 2004; Melero-Jerez et al., 2021). Demyelination with LPC was confirmed, after being removed from the medium, with a 55%–60% reduction in both the amount of myelin and its co-localization with neurofilaments. To study the remyelinating effect of the aptamer, we maintained the slices for 6 dpl, and increased myelin production was evident in LPC slices that received ApTOLL than in those that received the vehicle alone (Figure 6b,c). Moreover, treatment with ApTOLL resulted in a significantly higher proportion of remyelinated axons than when they were exposed to the vehicle alone (Figure 6b,d), the latter only showing a 22% increase over the control at 0 dpl (LPC + control 22.6 ± 3.0%, LPC + Veh 27.6 ± 6.8%: Student's *t*-test $P > 0.05$), whereas exposure to ApTOLL produced a 130% increase (LPC + control 22.6 ± 3.0%, LPC + ApTOLL 51.8 ± 6.7%: Student's *t*-test $P < 0.05$).

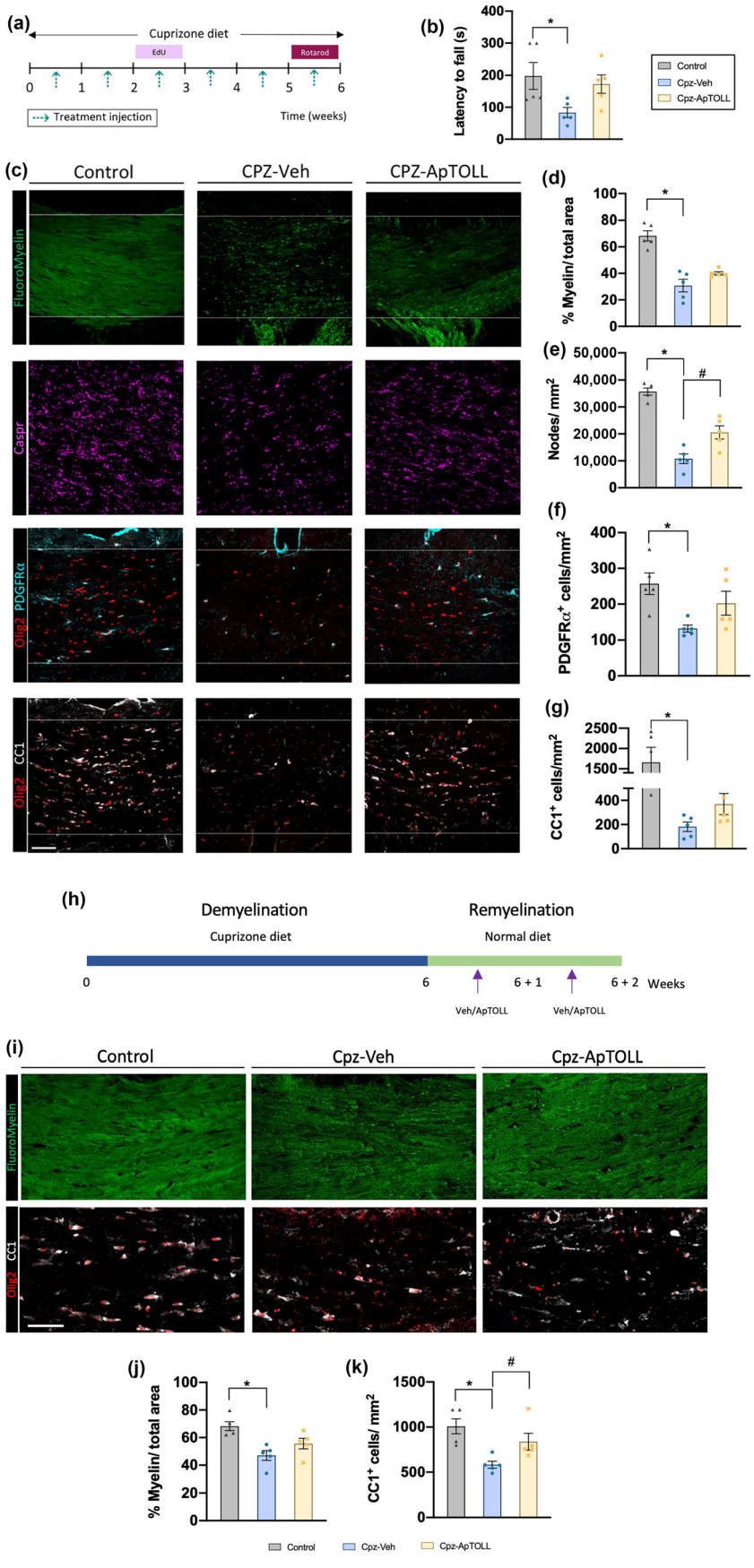

FIGURE 4 Myelin and oligodendrocytes increase in the CC of CPZ-ApTOLL mice. (a) Scheme of the experimental procedure for the demyelination study (n = 5). (b) Results from the rotarod assay performed at the end of 6 weeks. Animals that received ApTOLL weekly took longer to fall off the rod than the mice that received the vehicle alone. (c–g) Confocal images of the CC after receiving CPZ for 6 weeks and quantification of the staining for myelin (green, d), paranodes (magenta, e), OPCs (cyan, f) and mature oligodendrocytes (grey, g). A significant enhancement in myelin and in the number of oligodendrocytes was observed in CPZ-ApTOLL animals. (h) Scheme of the experimental procedure for the remyelination study (n = 5). Representative images (i) and quantifications for myelin (j) and mature oligodendrocytes (k) after cuprizone withdrawal. Scale bar: 60 μm in (c) and (i) and 20 μm in Caspr staining. The results of the one-way ANOVA test for multiple comparisons are represented by $^{*}P < 0.05$. An unpaired Student's *t*-test was used to compare pairs of conditions, represented by $^{\#}P < 0.05$.

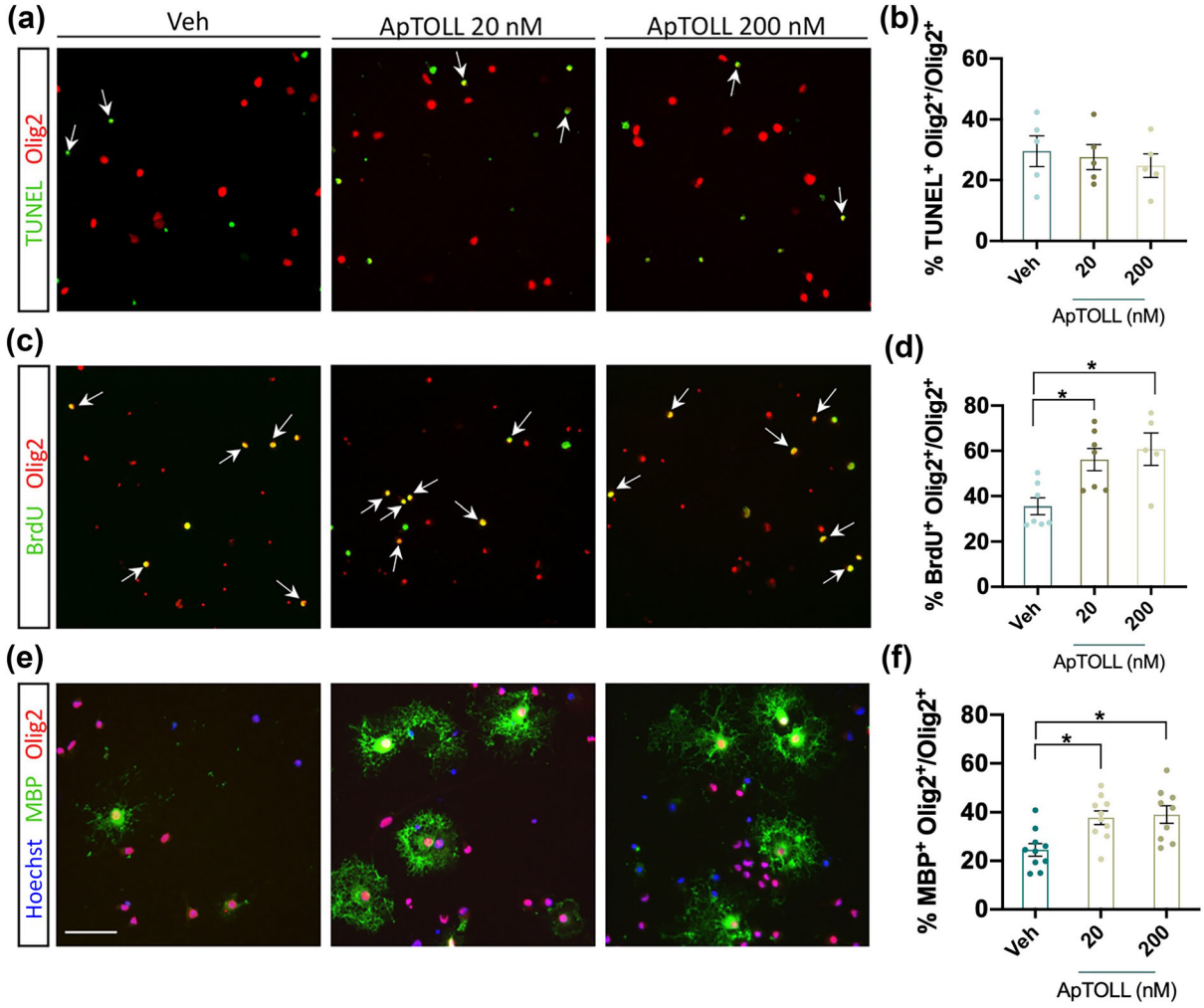

FIGURE 5 ApTOLL enhances murine OPC proliferation and differentiation. (a) Images of OPCs labelled for Olig2 (red) and apoptotic TUNEL-stained cells (green) taken under epifluorescence microscopy. (b) The graph shows the percentage of apoptotic $Olig2^+$ cells. There are no differences in the survival of cells under the different conditions (n = 5). (c) Images showing proliferating cells that express BrdU (green) taken under epifluorescence microscopy. (d) Histogram showing the proportion of $Olig2^+/BrdU^+$ cells. There is an increase with both doses of ApTOLL when compared to the vehicle alone (n = 7). (e) Representative fluorescence images of differentiated OPCs expressing MBP (green). (f) Graph showing the number of myelin-forming cells. There is an enhancement induced by ApTOLL in the culture medium (n = 10). Arrows indicate double-labelled cells. Scale bar: 50 µm. ApTOLL versus vehicle groups were compared using an unpaired Student's *t*-test, and the results are expressed as $^*P < 0.05$.

3.6 | ApTOLL enhances the maturation of haOPCs towards myelinating phenotypes and increases myelin production

Based on the data obtained from rat OPCs in vitro, we determined whether ApTOLL exerted a pro-myelinating effect in primary cultures of haOPCs isolated from non-tumour biopsies of the adult cerebral cortex. As described previously (Medina-Rodríguez et al., 2017), it was necessary to maintain these cells for at least 15 DIV to differentiate them. Exposure to ApTOLL (20 nM) gave rise to more mature oligodendrocytes ($CC1^+$) than when the OPCs were cultured in control conditions, and these differences were even more pronounced when 200-nM ApTOLL was used (Figure 7a,b). However, both treatments gave similar results in terms of the myelin proteins generated by these mature oligodendrocytes (measured as MBP^+ area) with respect to the total number of cells quantified in each field (Figure 7a,c). Together, these results show that, as seen with rodent cells, ApTOLL may have a direct effect on promoting the production of proteins needed for myelin formation by haOPCs, and they suggest that ApTOLL may be a suitable agent to directly promote effective remyelination in MS in addition to its anti-inflammatory activities.

4 | DISCUSSION AND CONCLUSIONS

The contribution of the inflammatory–immunological component to MS pathogenesis has been extensively demonstrated, and it is known that TLRs (including TLR4) play important roles in it (Andersson

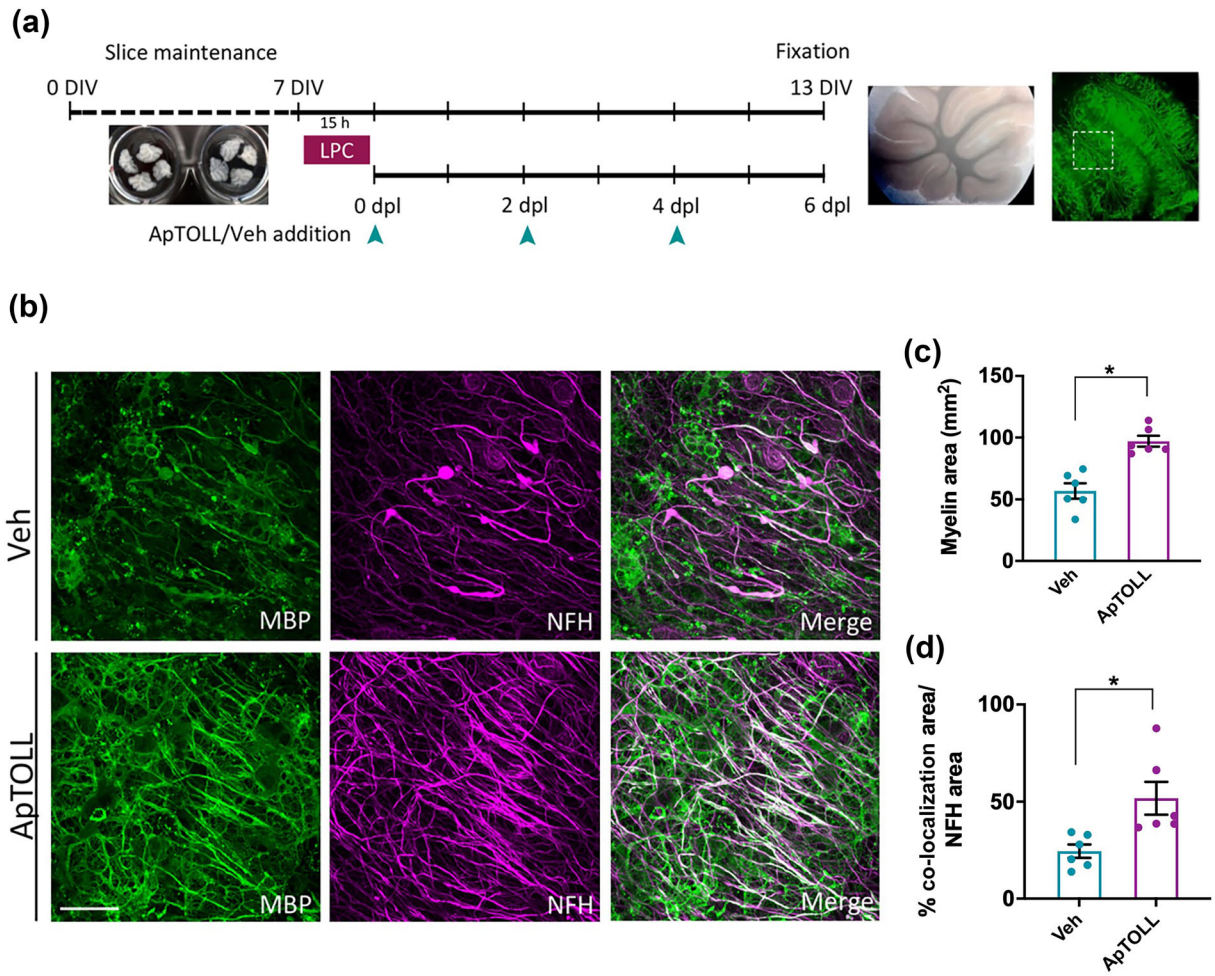

FIGURE 6 ApTOLL promotes remyelination ex vivo. (a) Scheme of the experimental procedure to maintain cerebellar slices in organotypic culture. (b) Representative images of the parallel fibres (NFH, magenta) present in the cerebellar samples and of myelin (MBP, green) under the different conditions after exposure to a demyelinating insult with LPC. Graphs show a significant increase in both the total myelin area (c) and co-localization with neurofilaments (d) in the LPC-lesioned slices treated with ApTOLL. Scale bar: 50 μm in (b). n = 6 independent experiments. An unpaired Student's *t* test was used and represented by $^{*}P < 0.05$.

et al., 2008; Gambuzza et al., 2011; Zhang et al., 2019). The new TLR4 antagonist aptamer (ApTOLL or 4FT-aptamer) is being studied in preclinical models and clinical trials to treat ischaemic stroke and myocardial infarction (Fernández et al., 2018; Hernández-Jiménez, Abad-Santos, Cotgreave, Gallego, Jilma, Flores, Jovin, Vivancos, Hernández-Pérez, et al., 2023; Hernández-Jiménez, Abad-Santos, Cotgreave, Gallego, Jilma, Flores, Jovin, Vivancos, Molina, et al., 2023; Hernández-Jiménez et al., 2022; Paz-García et al., 2023; Ramirez-Carracedo et al., 2020), and here, we propose that this aptamer can also be a promising candidate for the treatment of MS. Indeed, we not only reveal an anti-inflammatory response but also demonstrate its neuroprotective activity and direct promotion of OPC differentiation and myelin formation.

Aptamers are new therapeutic entities due to their high affinity and specificity, as well as their advantages over conventional drugs or antibodies (safety, stability, in vitro selection, ability to be modified without structural alterations, chemical manufacturing, etc.; Kanwar et al., 2015). Here, we show how a single injection of ApTOLL resulted in a significant recovery of clinical symptoms in the EAE model, which was associated with increased myelin and axonal preservation. Interestingly, our results show a U-shaped dose–response curve in the ability of ApTOLL to reduce clinical scores in the EAE model. U-shaped dose–response curves (also called hormesis) have been documented in numerous biological, toxicological and pharmacological investigations so far (Calabrese, 2018). Hormesis can be considered as an adaptive mechanism to compensate for any imbalance in homeostasis caused by exposure to factors that mediate intermittent mild stresses of biological, physical or chemical origin. There are different mechanisms underlying hormesis, and they can involve a wide range of biological pathways likely related to overcompensation responses including inflammation (Calabrese & Baldwin, 2001). For this reason, U-shaped responses raise important issues for toxicological risk assessment and in the establishment of clinical endpoints (Agathokleous & Calabrese, 2019). We detected maximal effects when ApTOLL was administered at the onset of clinical symptoms, consistent with the acute phase of EAE and the moment when the

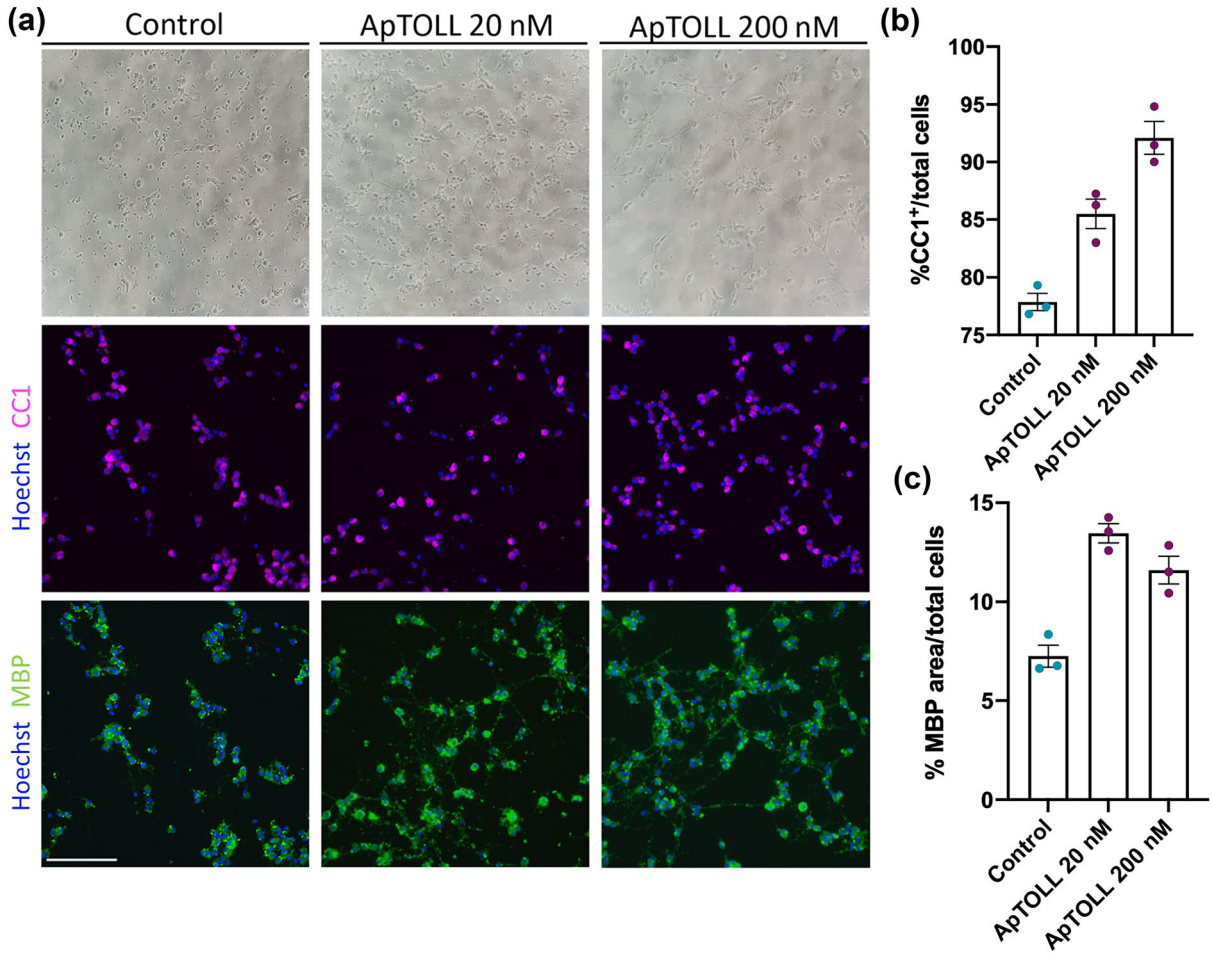

FIGURE 7 ApTOLL exerts a direct effect on the differentiation of OPCs from adult human biopsies. (a) Representative images of human mature oligodendrocytes expressing CC1 (magenta) and MBP (green). Enhanced numbers of mature cells (b) and an increase in the area occupied by MBP (c) are observed in the presence of ApTOLL. Scale bar: 50 μm in (a).

initial proinflammatory modulators are being released (Borjini et al., 2016). The aptamer notably reduced the number of microglia/macrophages in vivo. However, those cells that remain active could be participating in phagocytic functions of myelin or axonal debris (Rajbhandari et al., 2014), as suggested by the changes in the expression of different markers (CD68 and CD206) and also in their morphology, which is considered as a necessary process for proper remyelination (Franklin, 2002; Lubetzki et al., 2020). Hence, the treatment with ApTOLL in this MS model may produce a remarkable clinical improvement, which could be due to the modulation of an excessively strong immune response, preventing tissue damage. However, the effect of ApTOLL would not be limited to the inflammatory component. In this sense, we have observed a remarkable effect on the elements involved in the remyelination process, that is, on OPCs. This effect goes beyond the fact that ApTOLL decreases inflammatory conditions, to which elements of the oligodendroglial lineage are particularly sensitive (Li et al., 2014; Zhao et al., 2016). In a main demyelinating scenario with a minor inflammatory component such as the CPZ animal model of demyelination in vivo, treatment with ApTOLL significantly promoted the number of OPCs (better survival plus promoted proliferation) and mature oligodendrocytes and myelin distribution. Altogether, our observations could reflect the acceleration of spontaneous remyelination, which could mean a new therapeutic application of ApTOLL beyond the anti-inflammatory effect. This was corroborated in OPC primary cultures. We can conclude that this pro-myelinating effect of the aptamer would not be minor because it is known that, for successful remyelination, quiescent OPCs must actively proliferate and be properly recruited towards demyelinating areas (Franklin et al., 2021; Saitoh et al., 2022).

Nevertheless, it is not only important to increase the number of OPCs, but clinical benefits rely on their differentiation towards myelin-forming phenotypes. It has been argued that the proliferation and differentiation of OPCs are sequential events that cannot take place simultaneously (Plemel et al., 2013); however, these results are in line with others that show that the proliferation of OPCs and the maturation process can coexist (Melero-Jerez et al., 2021; Wu et al., 2014; Zhang et al., 2015). The present data from haOPCs strongly support that this would be the case in human MS. In spite of the remarkable heterogeneity of OPCs recently demonstrated (Hilscher et al., 2022; Jäkel et al., 2019), the present observations suggest that ApTOLL

effects on these cells do not vary according to age or species, which could help ulterior preclinical and clinical developments.

Finally, we showed that the treatment with ApTOLL promoted the coating of axons that had been demyelinated in organotypic cultures and then favoured remyelination. Previous data from various authors indicate that signalling pathways such as Wnt / **β-catenin** and **Akt** / **mammalian target of rapamycin** (mTOR) play important roles during the differentiation of OPCs and the myelination process (Dai et al., 2014; Ishii et al., 2019; Norrmén & Suter, 2013; Wang et al., 2021). These signalling pathways have been found to interact and mutually regulate NF-κB, a product of the TLR4 pathway (Gaesser & Fyffe-Maricich, 2016; Ma & Hottiger, 2016). However, the relation between these signalling pathways is still unknown, and it would be interesting to determine the concrete mechanisms by which ApTOLL can act in non-inflammatory cells such as oligodendrocytes.

Together, our current findings suggest a new therapeutic approach for the treatment of inflammatory and demyelinating diseases such as MS. The molecular nature of the aptamer ensures ApTOLL to exert a clear and safe anti-inflammatory effect, as well as indirect/direct neuroprotective and remyelinating effects. This confers advantages over other compounds. Importantly, ApTOLL also exerts a clear safety profile, as demonstrated in the first-in-human study (Hernández-Jiménez et al., 2022), as well as efficacy in reducing brain damage in stroke patients (Hernández-Jiménez, Abad-Santos, Cotgreave, Gallego, Jilma, Flores, Jovin, Vivancos, Hernández-Pérez, et al., 2023; Hernández-Jiménez, Abad-Santos, Cotgreave, Gallego, Jilma, Flores, Jovin, Vivancos, Molina, et al., 2023). This opens the door to future clinical trials with this aptamer in human MS patients.

AUTHOR CONTRIBUTIONS

B. Fernández Gómez: Data curation (equal); formal analysis (lead); investigation (lead); methodology (equal); writing—original draft (lead); writing—review and editing (equal). **M. A. Marchena:** Investigation (equal); methodology (equal); supervision (equal); writing-original draft (equal); writing—review and editing (equal). **D. Piñeiro:** resources (equal). **P. Gómez Martín:** Investigation (equal). **E. Sanchez:** Investigation (equal). **Y. Laó:** Investigation (equal). **G. Valencia:** Investigation (equal). **S. Nocera:** Investigation (equal); methodology (equal). **R. Benítez-Fernández:** Investigation (equal). **A. M. Castaño León:** Resources (equal). **A. Lagares:** Resources (equal). **M. Hernández Jiménez:** Conceptualization (equal); supervision (equal); validation (equal); writing—review and editing (equal). **F. de Castro:** Conceptualization (lead); funding acquisition (equal); project administration (lead); supervision (lead); validation (equal); writing—review and editing (lead); data curation (lead); formal analysis (equal); methodology (lead); investigation (equal); resources (lead); writing -original draft (equal).

ACKNOWLEDGEMENTS

This work was supported by the following grants and contracts to FdC: IND2018/BMD-9751 (Programa de Doctorados Industriales, Comunidad de Madrid, Spain); SAF2016-77575-R, PID2019-109858RB-I00, PID2022-143110OB-I00, EIN2020-112366 and RD16/0015/0019 (grant funded by the Spanish Ministerio de Ciencia Investigación e Innovación—MCIN/AEI/10.13039/501100011033 and by 'ERDF a way of making Europe' by the European Union), 2019AEP033 (from Consejo Superior de Investigaciones Científicas—CSIC, Spain), and a contract for technological support (20184174) from AptaTargets SL (Spain). BF-G is currently hired by AptaTargets SL; PG-M was contracted as Ayudante de Investigación (PEJ-2020-AI/BMD-18541), associated with the Fondo de Garantía Juvenil (call 2020), financed by Comunidad de Madrid (Spain) and now hired under Grant 2019AEP033; SN was hired under IND2018/BMD-9751 (to FdC); and YL has been contracted under RD16/0015/0019 and PID2019-109858RB-I00. We thank David Segarra and Mª Eugenia Zarabozo (AptaTargets SL) for their constant technological support, Laude Garmendia for her indispensable constant help at the animal facility (Instituto Cajal—CSIC), including the extra effort during COVID-19 pandemics, and Dr. Carolina Melero-Jerez (a former member of the FdC research group, currently working at JazzPharma, Spain) for the initial training of BF-G on the EAE animal model and different techniques at the laboratory.

CONFLICT OF INTEREST STATEMENT

The authors have no conflicts of interest.

DATA AVAILABILITY STATEMENT

The data that support the findings of this study are available from the corresponding author upon reasonable request.

DECLARATION OF TRANSPARENCY AND SCIENTIFIC RIGOUR

This Declaration acknowledges that this paper adheres to the principles for transparent reporting and scientific rigour of preclinical research as stated in the *BJP* guidelines for Design & Analysis, Immunoblotting and Immunochemistry, and Animal Experimentation and as recommended by funding agencies, publishers and other organizations engaged with supporting research.

ORCID

Fernando de Castro https://orcid.org/0000-0002-7018-8032

REFERENCES

Agathokleous, E., & Calabrese, E. J. (2019). Hormesis: The dose response for the 21st century: The future has arrived. *Toxicology*, *425*, 152249. https://doi.org/10.1016/j.tox.2019.152249

Alexander, S. P., Fabbro, D., Kelly, E., Mathie, A., Peters, J. A., Veale, E. L., Armstrong, J. F., Faccenda, E., Harding, S. D., Pawson, A. J., Southan, C., Davies, J. A., Beuve, A., Brouckaert, P., Bryant, C., Burnett, J. C., Farndale, R. W., Friebe, A., Garthwaite, J., … Waldman, S. A. (2021). The Concise Guide to PHARMACOLOGY 2021/22: Catalytic receptors. *British Journal of Pharmacology*, *178*-(Suppl 1), S264–S312. https://doi.org/10.1111/bph.15541

Alexander, S. P. H., Roberts, R. E., Broughton, B. R. S., Sobey, C. G., George, C. H., Stanford, S. C., Cirino, G., Docherty, J. R., Giembycz, M. A., Hoyer, D., Insel, P. A., Izzo, A. A., Ji, Y., MacEwan, D. J., Mangum, J., Wonnacott, S., & Ahluwalia, A. (2018). Goals and practicalities of immunoblotting and immunohistochemistry: A guide for submission to the British Journal of Pharmacology. *British*

Journal of Pharmacology, *175*(3), 407–411. https://doi.org/10.1111/bph.14112

Andersson, A., Covacu, R., Sunnemark, D., Danilov, A. I., Dal Bianco, A., Khademi, M., Wallström, E., Lobell, A., Brundin, L., Lassmann, H., & Harris, R. A. (2008). Pivotal advance: HMGB1 expression in active lesions of human and experimental multiple sclerosis. *Journal of Leukocyte Biology*, *84*(5), 1248–1255. https://doi.org/10.1189/jlb.1207844

Baufeld, C., O'Loughlin, E., Calcagno, N., Madore, C., & Butovsky, O. (2018). Differential contribution of microglia and monocytes in neurodegenerative diseases. *Journal of Neural Transmission (Vienna, Austria: 1996)*, *125*(5), 809–826. https://doi.org/10.1007/s00702-017-1795-7

Birgbauer, E., Rao, T. S., & Webb, M. (2004). Lysolecithin induces demyelination in vitro in a cerebellar slice culture system. *Journal of Neuroscience Research*, *78*(2), 157–166. https://doi.org/10.1002/jnr.20248

Borjini, N., Fernández, M., Giardino, L., & Calzà, L. (2016). Cytokine and chemokine alterations in tissue, CSF, and plasma in early presymptomatic phase of experimental allergic encephalomyelitis (EAE), in a rat model of multiple sclerosis. *Journal of Neuroinflammation*, *13*(1), 291. https://doi.org/10.1186/s12974-016-0757-6

Bsibsi, M., Ravid, R., Gveric, D., & van Noort, J. M. (2002). Broad expression of toll-like receptors in the human central nervous system. *Journal of Neuropathology and Experimental Neurology*, *61*(11), 1013–1021. https://doi.org/10.1093/jnen/61.11.1013

Calabrese, E. J. (2018). Hormesis: Path and progression to significance. *International Journal of Molecular Sciences*, *19*(10), 2871. https://doi.org/10.3390/ijms19102871

Calabrese, E. J., & Baldwin, L. A. (2001). Hormesis: U-shaped dose responses and their centrality in toxicology. *Trends Pharmacol Sci*, *22*(6), 285–291. https://doi.org/10.1016/s0165-6147(00)01719-3.

Curtis, M. J., Alexander, S. P. H., Cirino, G., George, C. H., Kendall, D. A., Insel, P. A., Izzo, A. A., Ji, Y., Panettieri, R. A., Patel, H. H., Sobey, C. G., Stanford, S. C., Stanley, P., Stefanska, B., Stephens, G. J., Teixeira, M. M., Vergnolle, N., & Ahluwalia, A. (2022). Planning experiments: Updated guidance on experimental design and analysis and their reporting III. *British Journal of Pharmacology*, *179*(15), 3907–3913. https://doi.org/10.1111/bph.15868

Dai, J., Bercury, K. K., & Macklin, W. B. (2014). Interaction of mTOR and Erk1/2 signaling to regulate oligodendrocyte differentiation. *Glia*, *62*(12), 2096–2109. https://doi.org/10.1002/glia.22729

de Castro, F., Bribián, A., & Ortega, M. C. (2013). Regulation of oligodendrocyte precursor migration during development, in adulthood and in pathology. *Cellular and Molecular Life Sciences*, *70*(22), 4355–4368. https://doi.org/10.1007/s00018-013-1365-6.

Dincman, T. A., Beare, J. E., Ohri, S. S., & Whittemore, S. R. (2012). Isolation of cortical mouse oligodendrocyte precursor cells. *Journal of Neuroscience Methods*, *209*(1), 219–226. https://doi.org/10.1016/j.jneumeth.2012.06.017

Fernández, G., Moraga, A., Cuartero, M. I., García-Culebras, A., Peña-Martínez, C., Pradillo, J. M., Hernández-Jiménez, M., Sacristán, S., Ayuso, M. I., Gonzalo-Gobernado, R., Fernández-López, D., Martín, M. E., Moro, M. A., González, V. M., & Lizasoain, I. (2018). TLR4-binding DNA aptamers show a protective effect against acute stroke in animal models. *Molecular Therapy: The Journal of the American Society of Gene Therapy*, *26*(8), 2047–2059. https://doi.org/10.1016/j.ymthe.2018.05.019

Franklin, R. J. (2002). Why does remyelination fail in multiple sclerosis? *Nature Reviews. Neuroscience*, *3*(9), 705–714. https://doi.org/10.1038/nrn917

Franklin, R. J. M., & ffrench-Constant, C. (2017). Regenerating CNS myelin—From mechanisms to experimental medicines. *Nature Reviews. Neuroscience*, *18*(12), 753–769. https://doi.org/10.1038/nrn.2017.136

Franklin, R. J. M., Frisén, J., & Lyons, D. A. (2021). Revisiting remyelination: Towards a consensus on the regeneration of CNS myelin. *Seminars in Cell & Developmental Biology*, *116*, 3–9. https://doi.org/10.1016/j.semcdb.2020.09.009

Gaesser, J. M., & Fyffe-Maricich, S. L. (2016). Intracellular signaling pathway regulation of myelination and remyelination in the CNS. *Experimental Neurology*, *283*(Pt B), 501–511. https://doi.org/10.1016/j.expneurol.2016.03.008

Gambuzza, M., Licata, N., Palella, E., Celi, D., Foti Cuzzola, V., Italiano, D., Marino, S., & Bramanti, P. (2011). Targeting toll-like receptors: Emerging therapeutics for multiple sclerosis management. *Journal of Neuroimmunology*, *239*(1–2), 1–12. https://doi.org/10.1016/j.jneuroim.2011.08.010

Gharagozloo, M., Mace, J. W., & Calabresi, P. A. (2022). Animal models to investigate the effects of inflammation on remyelination in multiple sclerosis. *Frontiers in Molecular Neuroscience*, *15*, 995477. https://doi.org/10.3389/fnmol.2022.995477

Gudi, V., Gingele, S., Skripuletz, T., & Stangel, M. (2014). Glial response during cuprizone-induced de- and remyelination in the CNS: Lessons learned. *Frontiers in Cellular Neuroscience*, *8*, 73. https://doi.org/10.3389/fncel.2014.00073

Gudi, V., Moharregh-Khiabani, D., Skripuletz, T., Koutsoudaki, P. N., Kotsiari, A., Skuljec, J., Trebst, C., & Stangel, M. (2009). Regional differences between grey and white matter in cuprizone induced demyelination. *Brain Research*, *1283*, 127–138. https://doi.org/10.1016/j.brainres.2009.06.005

Hayakawa, K., Pham, L. D., Seo, J. H., Miyamoto, N., Maki, T., Terasaki, Y., Sakadžić, S., Boas, D., van Leyen, K., Waeber, C., Kim, K. W., Arai, K., & Lo, E. H. (2016). CD200 restrains macrophage attack on oligodendrocyte precursors via toll-like receptor 4 downregulation. *Journal of Cerebral Blood Flow and Metabolism: Official Journal of the International Society of Cerebral Blood Flow and Metabolism*, *36*(4), 781–793. https://doi.org/10.1177/0271678X15606148

Hernández-Jiménez, M., Abad-Santos, F., Cotgreave, I., Gallego, J., Jilma, B., Flores, A., Jovin, T. G., Vivancos, J., Hernández-Pérez, M., Molina, C. A., Montaner, J., Casariego, J., Dalsgaard, M., Liebeskind, D. S., Cobo, E., Castellanos, M., Portela, P. C., Masjuán, J., Moniche, F., … Ribo, M. (2023). Safety and efficacy of ApTOLL in patients with ischemic stroke undergoing endovascular treatment: A phase 1/2 randomized clinical trial. *JAMA Neurology*, *80*(8), 779–788. https://doi.org/10.1001/jamaneurol.2023.1660

Hernández-Jiménez, M., Abad-Santos, F., Cotgreave, I., Gallego, J., Jilma, B., Flores, A., Jovin, T. G., Vivancos, J., Molina, C. A., Montaner, J., Casariego, J., Dalsgaard, M., Hernández-Pérez, M., Liebeskind, D. S., Cobo, E., & Ribo, M. (2023). APRIL: A double-blind, placebo-controlled, randomized, Phase Ib/IIa clinical study of ApTOLL for the treatment of acute ischemic stroke. *Frontiers in Neurology*, *14*, 1127585. https://doi.org/10.3389/fneur.2023.1127585

Hernández-Jiménez, M., Martín-Vílchez, S., Ochoa, D., Mejía-Abril, G., Román, M., Camargo-Mamani, P., Luquero-Bueno, S., Jilma, B., Moro, M. A., Fernández, G., Piñeiro, D., Ribó, M., González, V. M., Lizasoain, I., & Abad-Santos, F. (2022). First-in-human phase I clinical trial of a TLR4-binding DNA aptamer, ApTOLL: Safety and pharmacokinetics in healthy volunteers. *Molecular Therapy. Nucleic Acids*, *28*, 124–135. https://doi.org/10.1016/j.omtn.2022.03.005

Hibbits, N., Pannu, R., Wu, T. J., & Armstrong, R. C. (2009). Cuprizone demyelination of the corpus callosum in mice correlates with altered social interaction and impaired bilateral sensorimotor coordination. *ASN Neuro*, *1*(3), e00013. https://doi.org/10.1042/AN20090032

Hilscher, M. M., Langseth, C. M., Kukanja, P., Yokota, C., Nilsson, M., & Castelo-Branco, G. (2022). Spatial and temporal heterogeneity in the lineage progression of fine oligodendrocyte subtypes. *BMC Biology*, *20*(1), 122. https://doi.org/10.1186/s12915-022-01325-z

Ishii, A., Furusho, M., Macklin, W., & Bansal, R. (2019). Independent and cooperative roles of the Mek/ERK1/2-MAPK and PI3K/Akt/mTOR pathways during developmental myelination and in adulthood. *Glia*, *67*(7), 1277–1295. https://doi.org/10.1002/glia.23602

Jäkel, S., Agirre, E., Mendanha Falcão, A., van Bruggen, D., Lee, K. W., Knuesel, I., Malhotra, D., ffrench-Constant, C., Williams, A., & Castelo-Branco, G. (2019). Altered human oligodendrocyte heterogeneity in multiple sclerosis. *Nature*, *566*(7745), 543–547. https://doi.org/10.1038/s41586-019-0903-2

Kanwar, J. R., Roy, K., Maremanda, N. G., Subramanian, K., Veedu, R. N., Bawa, R., & Kanwar, R. K. (2015). Nucleic acid-based aptamers: Applications, development and clinical trials. *Current Medicinal Chemistry*, *22*(21), 2539–2557. https://doi.org/10.2174/0929867322666150227144909

Kerfoot, S. M., Long, E. M., Hickey, M. J., Andonegui, G., Lapointe, B. M., Zanardo, R. C., Bonder, C., James, W. G., Robbins, S. M., & Kubes, P. (2004). TLR4 contributes to disease-inducing mechanisms resulting in central nervous system autoimmune disease. *Journal of Immunology (Baltimore, Md.: 1950)*, *173*(11), 7070–7077. https://doi.org/10.4049/jimmunol.173.11.7070

Kipp, M., Clarner, T., Dang, J., Copray, S., & Beyer, C. (2009). The cuprizone animal model: New insights into an old story. *Acta Neuropathologica*, *118*(6), 723–736. https://doi.org/10.1007/s00401-009-0591-3

Kremer, D., Küry, P., & Dutta, R. (2015). Promoting remyelination in multiple sclerosis: Current drugs and future prospects. *Multiple Sclerosis (Houndmills, Basingstoke, England)*, *21*(5), 541–549. https://doi.org/10.1177/1352458514566419

Lassmann, H., & Bradl, M. (2017). Multiple sclerosis: Experimental models and reality. *Acta Neuropathologica*, *133*(2), 223–244. https://doi.org/10.1007/s00401-016-1631-4

Li, J. Y., Liu, Y., Gao, X. X., Gao, X., & Cai, H. (2014). TLR2 and TLR4 signaling pathways are required for recombinant *Brucella abortus* BCSP31-induced cytokine production, functional upregulation of mouse macrophages, and the Th1 immune response in vivo and in vitro. *Cellular & Molecular Immunology*, *11*(5), 477–494. https://doi.org/10.1038/cmi.2014.28

Lilley, E., Stanford, S. C., Kendall, D. E., Alexander, S. P. H., Cirino, G., Docherty, J. R., George, C. H., Insel, P. A., Izzo, A. A., Ji, Y., Panettieri, R. A., Sobey, C. G., Stefanska, B., Stephens, G., Teixeira, M., & Ahluwalia, A. (2020). ARRIVE 2.0 and the British Journal of Pharmacology: Updated guidance for 2020. *British Journal of Pharmacology*, *177*(16), 3611–3616. https://doi.org/10.1111/bph.15178

Liu, T., Zhang, L., Joo, D., & Sun, S. C. (2017). NF-κB signaling in inflammation. *Signal Transduction and Targeted Therapy*, *2*, 17023. https://doi.org/10.1038/sigtrans.2017.23

Lubetzki, C., Zalc, B., Williams, A., Stadelmann, C., & Stankoff, B. (2020). Remyelination in multiple sclerosis: From basic science to clinical translation. *The Lancet. Neurology*, *19*(8), 678–688. https://doi.org/10.1016/S1474-4422(20)30140-X

Ma, B., & Hottiger, M. O. (2016). Crosstalk between Wnt/β-catenin and NF-κB signaling pathway during inflammation. *Frontiers in Immunology*, *7*, 378. https://doi.org/10.3389/fimmu.2016.00378

Medina-Rodríguez, E. M., Bribián, A., Boyd, A., Palomo, V., Pastor, J., Lagares, A., Gil, C., Martínez, A., Williams, A., & de Castro, F. (2017). Promoting in vivo remyelination with small molecules: A neuroreparative pharmacological treatment for multiple sclerosis. *Scientific Reports*, *7*, 43545. https://doi.org/10.1038/srep43545

Melero-Jerez, C., Fernández-Gómez, B., Lebrón-Galán, R., Ortega, M. C., Sánchez-de Lara, I., Ojalvo, A. C., Clemente, D., & de Castro, F. (2021). Myeloid-derived suppressor cells support remyelination in a murine model of multiple sclerosis by promoting oligodendrocyte precursor cell survival, proliferation, and differentiation. *Glia*, *69*(4), 905–924. https://doi.org/10.1002/glia.23936

Norrmén, C., & Suter, U. (2013). Akt/mTOR signalling in myelination. *Biochemical Society Transactions*, *41*(4), 944–950. https://doi.org/10.1042/BST20130046

Orihuela, R., McPherson, C. A., & Harry, G. J. (2016). Microglial M1/M2 polarization and metabolic states. *British Journal of Pharmacology*, *173*(4), 649–665. https://doi.org/10.1111/bph.13139

Paolicelli, R. C., Sierra, A., Stevens, B., Tremblay, M. E., Aguzzi, A., Ajami, B., Amit, I., Audinat, E., Bechmann, I., Bennett, M., Bennett, F., Bessis, A., Biber, K., Bilbo, S., Blurton-Jones, M., Boddeke, E., Brites, D., Brône, B., Brown, G. C., … Wyss-Coray, T. (2022). Microglia states and nomenclature: A field at its crossroads. *Neuron*, *110*(21), 3458–3483. https://doi.org/10.1016/j.neuron.2022.10.020

Paz-García, M., Povo-Retana, A., Jaén, R. I., Prieto, P., Peraza, D. A., Zaragoza, C., Hernandez-Jimenez, M., Pineiro, D., Regadera, J., García-Bermejo, M. L., Rodríguez-Serrano, E. M., Sánchez-García, S., Moro, M. A., Lizasoaín, I., Delgado, C., Valenzuela, C., & Boscá, L. (2023). Beneficial effect of TLR4 blockade by a specific aptamer antagonist after acute myocardial infarction. *Biomedicine & Pharmacotherapy = Biomedecine & Pharmacotherapie*, *158*, 114214. https://doi.org/10.1016/j.biopha.2023.114214

Percie du Sert, N., Hurst, V., Ahluwalia, A., Alam, S., Avey, M. T., Baker, M., Browne, W. J., Clark, A., Cuthill, I. C., Dirnagl, U., Emerson, M., Garner, P., Holgate, S. T., Howells, D. W., Karp, N. A., Lazic, S. E., Lidster, K., MacCallum, C. J., Macleod, M., … Würbel, H. (2020). The ARRIVE guidelines 2.0: Updated guidelines for reporting animal research. *British Journal of Pharmacology*, *177*(16), 3617–3624. https://doi.org/10.1111/bph.15193

Plemel, J. R., Manesh, S. B., Sparling, J. S., & Tetzlaff, W. (2013). Myelin inhibits oligodendroglial maturation and regulates oligodendrocytic transcription factor expression. *Glia*, *61*(9), 1471–1487. https://doi.org/10.1002/glia.22535

Rajbhandari, L., Tegenge, M. A., Shrestha, S., Ganesh Kumar, N., Malik, A., Mithal, A., Hosmane, S., & Venkatesan, A. (2014). Toll-like receptor 4 deficiency impairs microglial phagocytosis of degenerating axons. *Glia*, *62*(12), 1982–1991. https://doi.org/10.1002/glia.22719

Ramirez-Carracedo, R., Tesoro, L., Hernandez, I., Diez-Mata, J., Piñeiro, D., Hernandez-Jimenez, M., Zamorano, J. L., & Zaragoza, C. (2020). Targeting TLR4 with ApTOLL improves heart function in response to coronary ischemia reperfusion in pigs undergoing acute myocardial infarction. *Biomolecules*, *10*(8), 1167. https://doi.org/10.3390/biom10081167

Saitoh, S. S., Tanabe, S., & Muramatsu, R. (2022). Circulating factors that influence the central nervous system remyelination. *Current Opinion in Pharmacology*, *62*, 130–136. https://doi.org/10.1016/j.coph.2021.12.001

Skripuletz, T., Lindner, M., Kotsiari, A., Garde, N., Fokuhl, J., Linsmeier, F., Trebst, C., & Stangel, M. (2008). Cortical demyelination is prominent in the murine cuprizone model and is strain-dependent. *The American Journal of Pathology*, *172*(4), 1053–1061. https://doi.org/10.2353/ajpath.2008.070850

Taylor, D. L., Pirianov, G., Holland, S., McGinnity, C. J., Norman, A. L., Reali, C., Diemel, L. T., Gveric, D., Yeung, D., & Mehmet, H. (2010). Attenuation of proliferation in oligodendrocyte precursor cells by activated microglia. *Journal of Neuroscience Research*, *88*(8), 1632–1644. https://doi.org/10.1002/jnr.22335

Trapp, B. D., & Nave, K. A. (2008). Multiple sclerosis: An immune or neurodegenerative disorder? *Annual Review of Neuroscience*, *31*, 247–269. https://doi.org/10.1146/annurev.neuro.30.051606.094313

Wang, H., Liu, M., Ye, Z., Zhou, C., Bi, H., Wang, L., Zhang, C., Fu, H., Shen, Y., Yang, J. J., Hu, Y., & Chen, G. (2021). Akt regulates Sox10 expression to control oligodendrocyte differentiation via phosphorylating FoxO1. *The Journal of Neuroscience: The Official Journal of the Society for Neuroscience*, *41*(39), 8163–8180. https://doi.org/10.1523/JNEUROSCI.2432-20.2021

Wu, X., Qu, X., Zhang, Q., Dong, F., Yu, H., Yan, C., Qi, D., Wang, M., Liu, X., & Yao, R. (2014). Quercetin promotes proliferation and differentiation of oligodendrocyte precursor cells after oxygen/glucose deprivation-induced injury. *Cellular and Molecular Neurobiology*, *34*(3), 463–471. https://doi.org/10.1007/s10571-014-0030-4

Young, K., & Morrison, H. (2018). Quantifying microglia morphology from photomicrographs of immunohistochemistry prepared tissue using ImageJ. *Journal of Visualized Experiments: JoVE*, *136*, 57648. https://doi.org/10.3791/57648

Zhang, H., Wang, D., Sun, J., Wang, Y., Wu, S., & Wang, J. (2022). Huperzine—A improved animal behavior in cuprizone-induced mouse model by alleviating demyelination and neuroinflammation. *International Journal of Molecular Sciences*, *23*(24), 16182. https://doi.org/10.3390/ijms232416182

Zhang, J., Zhang, Z. G., Li, Y., Ding, X., Shang, X., Lu, M., Elias, S. B., & Chopp, M. (2015). Fingolimod treatment promotes proliferation and differentiation of oligodendrocyte progenitor cells in mice with experimental autoimmune encephalomyelitis. *Neurobiology of Disease*, *76*, 57–66. https://doi.org/10.1016/j.nbd.2015.01.006

Zhang, Z. M., Wang, Y. C., Chen, L., & Li, Z. (2019). Protective effects of the suppressed NF-κB/TLR4 signaling pathway on oxidative stress of lung tissue in rat with acute lung injury. *The Kaohsiung Journal of Medical Sciences*, *35*(5), 265–276. https://doi.org/10.1002/kjm2.12065

Zhao, Y., Zhao, Y., Zhang, M., Zhao, J., Ma, X., Huang, T., Pang, H., Li, J., & Song, J. (2016). Inhibition of TLR4 signalling-induced inflammation attenuates secondary injury after diffuse axonal injury in rats. *Mediators of Inflammation*, *2016*, 4706915. https://doi.org/10.1155/2016/4706915

Zhou, J., & Rossi, J. (2017). Aptamers as targeted therapeutics: Current potential and challenges. *Nature Reviews. Drug Discovery*, *16*(3), 181–202. https://doi.org/10.1038/nrd.2016.199

SUPPORTING INFORMATION

Additional supporting information can be found online in the Supporting Information section at the end of this article.

How to cite this article: Fernández-Gómez, B., Marchena, M. A., Piñeiro, D., Gómez-Martín, P., Sánchez, E., Laó, Y., Valencia, G., Nocera, S., Benítez-Fernández, R., Castaño-León, A. M., Lagares, A., Hernández-Jiménez, M., & F. de Castro (2024). ApTOLL: A new therapeutic aptamer for cytoprotection and (re)myelination after multiple sclerosis. *British Journal of Pharmacology*, 1–19. https://doi.org/10.1111/bph.16399